DOI: https://doi.org/10.24297/jap.v23i.9737

Preliminary design tasks for prototyping Self Sustaining Power Machines on Mars using local resources

Ramon Ferreiro Garcia

Former, Prof. Emeritus at the University of A Coruña, Spain, https://www.udc.es

ramon.ferreiro@udc.es

Abstract

This paper presents a preliminary design task to implement a group of machine prototypes capable of generating energy using the natural resources of Mars planet atmosphere. These prototypes are based on disruptive state of the art technologies particularly characterized by using pull forces achieved by cooling an appropriated thermal working fluid in the heat-work conversion interactions. Due to these groundbreaking characteristics, the machine functions as a hybrid isolated system. It operates both as an isolated system in relation to heat sources and sinks, and as a hybrid isolated system in its capacity to generate useful output energy for any energy-consuming application. This machine marks a significant advancement in combined cycles (CC), incorporating a Reversed Brayton Cycle (RBC) and a Self-Sustaining Power Machine (SSPM) of this kind. By combining these thermal engines, the technology enables operation without reliance on either an external heat source or heat sink, challenging traditional thermodynamic principles.

A group of prototypes design tasks based on the case study considers a combined cycle (CC) based on the combination of a heat pump consisting of a reverse Brayton cycle and a self-sustaining power machine (SSPM) is proposed to demonstrate these capabilities. The CC prototype consisting of a RBC and a SSPM was evaluated through the referred case study with argon for the RBC while using argon, air, nitrogen and carbon dioxide as real thermal working fluids (TWFs) for the cascaded PUs of the SSPM. Results depicted in Tables 16-18-20-22 and 23 indicate that the proposed CC operating equipped with a SSPMs composed by 6 PUs operating on a VsVs cycle achieved a total acceptable amounts of self-sufficient output net work.

Keywords: Self heat source, Self heat sink, Self-sustaining power machines, Self-heat power supply, In-situ utilization resources, and Mars atmosphere resources

Nomenclature related to general SSPMs

Acronyms	**Description/Context**
CF	Carnot Factor: CF=(qi-qo)/qi = $(T_H-T_L)/T_H$
Cont.	Contraction: a form of compression (volume reduction) achieved by cooling a TWF which gives rise to a pull force
CTF	Cooling Transfer Fluid (conventionally, thermal oil)
EM	electromagnetic
EP	Electric Power
Exp.	Expansion: a form of expansion (volume increase) achieved by heating a TWF which gives rise to a push force
FCF	Forced convection fan (recirculation fan of the TWF)
FP	Feed pump (feed compressor of the TWF)
Gen	Electric Power Generator: alternator or generator
HTF	Heating Transfer Fluid (conventionally, thermal oil)
Is_eff	Isentropic efficiency: (open processes). A coefficient of losses inherent to real gas expansion or compression
MT	Metric Tons: a metric Ton = 1000 kg
LF	Losses factor (include thermo-mechanical and thermo-hydraulic losses)
PP	Power Plant: a group of PUs coupled in cascade
PU	Power Unit operating with the thermal cycle sVsVs or VsVs cycle
RF	Heat recovery factor (includes heat transfer losses and leaks)

RIT	Ratio of Isochoric low to high temperatures [T_L/T_H], [T_1/T_3] for sVsVs, and [T_1/T_2] for VsVs,
SSI	Self-Sustaining Index: means the net free energy as % : [$SSI = (\eta_{th} - 100)/100$]
SSHS	Self-Sustaining Heat Supply
SEP	Self-Electric Power: SEP ≈ SSI (net mechanical power ≈ net electrical power)
sp	State point of any stationary point state of a thermal cycle
SSPM	Self-Sustaining Power Machine, Self-Sufficient Power Machine
SSPP	Self-Sustaining Power Plant, Self-Sufficient Power Plant
sVsVs	Cycle with the sequential processes: [isentropic-adiabatic (s), Isochoric (V), s,V,s]
TWF	Thermal Working Fluid
VsVs	Cycle with the sequential processes: [isochoric (V), isentropic-adiabatic (s), V, s]
CC	Combine Cycle
RBC	Reversed Brayton Cycle
FLT,	First law of thermodynamics
SLT,	Second law of thermodynamics
HIS.	Hybrid Isolated System
SHSk	Self heat sink
SHS	Self heat source
SHSk	Self heat sink
SSPM	Self-sustaining power machines
SHPS	Self-self-heat power supply
ISUR	In-situ utilization resources
MAR	Mars atmosphere resources
Symbols/units	***description***
p(bar)	pressure
q_i(kJ/kg)	specific heat in to a cycle process
q_{i23} (kJ/kg)	Input heat to cycle process 2-3
q_o(kJ/kg)	specific heat out from a cycle process
q_{o41} (kJ/kg)	output heat from cycle process 4-1 in a VsVs cycle
q_{rec}	Recovered heat from cycle process 4-1 in a VsVs cycle
Cp(kJ/kg-K)	specific heat capacity at constant pressure
Cv(kJ/kg-K)	specific heat capacity at constant volume
s(kJ/kg-K)	specific entropy
h(kJ/kg)	specific enthalpy
T(K)	temperature
T_H(K)	top cycle temperature
T_L(K)	bottoming cycle temperature
u(kJ/kg)	specific internal energy
v(m^3/kg)	specific volume

$V(m^3)$	volume
w(kJ/kg)	specific work
w_i(kJ/kg)	specific work input
w_{iFP}(kJ/kg)	Work added to drive the feed pump responsible to transfer the TWF
w_o(kJ/kg)	specific work out
w_{oexp} (kJ/kg)	Output expansion work due to previously added heat
w_{ocont} (kJ/kg)	Output contraction work due to previously extracted heat
w_{oexp23} (kJ/kg)	Output expansion work w_{o23} due to previously added heat
$w_{ocont41}$ (kJ/kg)	Output contraction work w_{o41} due to previously extracted heat
w_n (kJ/kg)	Net useful work ($w_{oexp} + w_{ocont}$) = ($w_{o23} + w_{o41}$)
wnT (kJ/kg)	Total net work (RBC work + Cascaded VsVs cycles works)
q_{rec}/PUi[kJ/kg]	Heat recovered from every PU from cooling cycles processes
T_{q_rec}/PUi [K]	Temperature of the heat recovered from cooling cycles processes in every PU
η_{th} (%)	Cycle thermal efficiency [w_n/qi]

Nomenclature related to Mars data, characteristics and activities

Acronym	**Full Form**	**Description/Context**
RDAC	Reciprocating Double-Acting Cylinder	A type of actuator used in thermal machines for contraction-based work.
PU	Power Unit	A system capable of generating power through thermal contraction/expansion.
SSPM	Self-Sustaining Power Machine	A power generation system that operates without external energy input, using local resources (e.g., Martian atmosphere).
ISRU	In-Situ Resource Utilization	The practice of collecting and processing Martian resources (e.g., CO_2, water) for fuel, life support, and construction.
MOXIE	Mars Oxygen In-Situ Resource Utilization Experiment	A NASA experiment on the Perseverance rover that produces oxygen from Martian CO_2.
SOEC	Solid Oxide Electrolysis Cell	A high-temperature electrolysis method for splitting CO_2 into O_2 and CO.
PSA	Pressure Swing Adsorption	A gas separation technique that uses pressure changes to adsorb/desorb gases (e.g., CO_2 capture).
MAHOSS	Mars Aromatic Hydrocarbon and Olefin Synthesis System	A method for producing fuel from Martian atmospheric CO_2.
HERA	Human Exploration Research Analog	A NASA habitat simulation for studying radiation shielding and crew health.
ESA	European Space Agency	The European counterpart to NASA, involved in Mars exploration research.

Nomenclature related to Mars data, characteristics and activities

Acronym	Full Form	Description/Context
SA	Synthetic Air	Clean air composed in situ of oxygen and nitrogen in breathable proportions and conditions, including the degree of humidity.
AI	Artificial Intelligence	Used for data approximation (e.g., Martian atmospheric composition).
RSLs	Recurring Slope Lines	Seasonal dark streaks on Mars possibly linked to liquid brine flows.
C4 Plants	-special category of Plants	Plants with a carbon-concentrating photosynthesis mechanism (e.g., corn).
CFCs	Chlorofluorocarbons	Potentially used in terraforming to thicken Mars' atmosphere.
CCs	Combined Cycles	In this work is a combination of thermal cycles: RBC and SSPM,
RBS-SSPM	a combination between a RBC and SSPM cycles	a RBC operating as power source and sink, while SSPM use it as power source and sink.

1 Introduction

To explore, exploit, and transform or manufacture a habitable environment for Martian resources, both those of its atmosphere and subsurface mineral resources [1-4], a production structure based on automated, self-sufficient, and/or autonomous manufacturing processes that require significant electrical power consumption is required. Likewise, environments adapted to plant and animal life must be protected from both solar and cosmic radiation [5-7], which entails significant electrical consumption.

Some of the most common intensive electricity consumers include:

Reusable Rockets for takeoff using low-cost liquid compressed and further reheated supercritical CO2 propulsion, heated by means of in-situ (on board) by means of electrical resistance (tungsten), magnetic induction or microwaves. Mainly for low-orbit takeoff,

Light helicopters and drones,

Autonomous transport vehicles, cranes, tracks, minerals-processing tools,

Drilling machines, excavators, tunnel boring machines, or backhoe loaders,

Casting of ferromagnetic metals and alloys,

Manufacture of utensils and tools with ferromagnetic materials,

Brick firing phase for the construction of anti-radiation barriers and habitats equipped with artificial light and all necessary services.

Therefore, given the recognized need to produce as much electrical energy as necessary autonomously, we propose to find disruptive and viable technical solutions, without which any attempt to colonize Mars would de facto represent a major failure for humanity.

So, given the meteorological conditions on Mars, characterized by an average minimum temperature below 270 K, we have a heat sink that significantly aids the production of electrical energy.

Even using this advantage, we still face the challenge of producing electrical energy without using heat sources and a heat sink.

Three disruptive technological challenges must be addressed to implement efficient power units (PUs) capable of operating through thermal contraction based on vacuum under closed processes-based adiabatic-isentropic transformations, as described in [8-10], and optionally through contraction based on strictly isothermal closed processes. The first challenge is that a thermal machine must be capable of operating through the aforementioned thermal cycle. The second challenge is that the thermal cycles must be able to operate with strictly isothermal processes of both thermal expansion and contraction. The third challenge is that a thermal machine must develop highly effective forced thermal convection heat transfer media at the transfer rate required by the nominal power of each PU, where each PU is composed of a pair of RDACs equipped with associated heat transfer equipment.

Recent contributions have led to disruptive advances in power plants composed of groups of power units coupled in cascade, operating through thermal cycles characterized by performing work due to the expansion and contraction of the thermal working fluid, as referenced in [11-14] and [16-17]. Expansion is achieved by adding heat, while contraction is achieved by extracting heat. Studies for designing and prototyping such power plants have been conducted using real gases as working fluids, with data obtained from E. W. Lemmon et al [15].

The focus of these advances is on improving the performance of SSPMs by employing disruptive heat regeneration techniques in the PUs, utilizing cascade heat recovery to achieve significantly higher efficiencies compared to conventional technologies. The prototyping tasks for the studied cases are covered by patents referenced in [19-21].

2 On the estimated resources of Mars with the help of AI.

This section considers the most relevant aspects related to the extraction and processing tasks expected on Mars. This refers to the estimation of the amount of energy required to carry out such challenges. These processing tasks, apart from the ability to supply sufficient energy at any required location and at any time, include autonomous operations and unlimited autonomy.

The responsibility for supplying energy from 50 MW-type power supplies that meet the aforementioned requirements can only be met by two technologies:

-- State-of-the-art self-sustaining nuclear reactors with a charge for at least half a century,

-- Self-Sustaining Power Machines (SSPMs) that require no external energy, are environmentally friendly, and are transportable to the application sites.

The choice between the two possible options is clear:

SSPMs are much cheaper, require lower maintenance costs, and are more reliable. For this reason, this study focuses on the use of Mars' natural resources, some of which exist in its atmosphere and are crucial for the implementation and operation of the proposed SSPMs.

2.1 Atmospheric composition and key characteristics of Mars

Disruptive energy supply techniques on Mars using local resources

Power supply technology on Mars is crucial because it is responsible for the following essential tasks and activities:

-- Implementation of electrical and/or mechanical power supply services for all applications requiring such resources.

-- Creating the autonomous industrial environment for the transformation and processing of resources necessary to provide the services required for the tasks at hand.

-- Exploration of mars surface to search for potential resources on masrs surface and

-- Exploiting the diversity of Martian useful resources and

-- Creating a sustainable and habitable habitat for plants and animals, including humans.

-- Storage, maintenance, and preservation of non-perishable materials to meet resource demands on exploration missions to other satellites of nearby planets, as well as assistance with travel inherent to cosmic exploration. Therefore, Table 1 shows a list of existing resources useful for taking the first steps related to colonizing the surface of Mars.

The transformation of natural resources on the Mars surface requires intensive energy consumption even when solar radiation is absent due to dark nights or cloud cover. Therefore, it is necessary to meet the high energy

demand to sustain the electro-intensive industry dedicated to the transformation of Mars' natural resources, regardless of the weather conditions in the location where the processing industry is located. This means that it is necessary a sustained energy production methodology and robust appropriated systems. Therefore, in order to meet such energy demand, the use of Self-Sustaining Power Machines (SSPM) is proposed with the planet's local resources. These machines are capable of supplying unlimited mechanical and/or electrical energy in intensity and time without the need for external energy resources,

The most relevant characteristics of Mars atmosphere are and potential necessary data focused on the Mars surface exploration is depicted in Table 1. Some of the resources mentioned are of vital importance for the exploration and exploitation of Mars.

Table 1: Atmospheric composition and key characteristics. Approximate data is achieved with the help of AI.

1. Atmospheric Composition (by volume):	
Carbon Dioxide (CO_2)	~95%
Nitrogen (N)	~2.8%
Argon (Ar)	~1.9–2%
Oxygen (O_2)	~0.17%
Carbon Monoxide (CO)	~0.06%
Trace gases:	
Water vapor (H_2O), methane (CH_4, sporadic), neon (Ne), krypton (Kr), xenon (Xe), ozone (O_3), hydrogen peroxide (H_2O_2).	
2. Physical Characteristics:	
Surface Pressure: ~6.36 mbar (0.6% of Earth's) – varies seasonally.	~6.36 mbar
Average Temperature:	~-60°C
ranging from ~-125°C at poles to +~20°C at equator.	
Density: ~0.02 kg/m^3 (much thinner than Earth's).	~0.02 kg/m^3
Gravity (m/s^2)	3.7
Scale Height: ~11 km (altitude where pressure drops by e).	~11 km
Wind Speeds:	2–7 m/s (gentle),
but dust storms can reach 30 m/s	
3. Chemical & Dynamic Features:	
CO_2 Dominance: Drives a weak greenhouse effect.	
Seasonal Changes: Polar CO_2 ice sublimates in summer, altering atmospheric pressure.	
Dust Storms: Can become global, heating the atmosphere and lifting fine particles.	
Methane (CH_4) Mystery: Detected intermittently—possible geological or biological origin (unconfirmed).	
Low Water Content: Mostly as ice or trace vapor; clouds of CO_2 & H_2O ice form.	
4. Implications:	
Too thin for liquid water (sublimates directly to vapor).	
No significant radiation shielding (due to lack of magnetic field & thin air).	
Affects spacecraft landings (requires aero braking & parachutes).	

Table 2: Heat capacity and adiabatic index of useful gases in the atmospheric composition of Mars

Gas names	**Proportional Abundance (%)**	**Total amount (MT) 25×10^{12}**	**Cp (kJ/kg K)**	**Adiabatic index γ=Cp/Cv**
Carbon dioxide (CO_2)	~95.3%	$0.953\times25\times10^{12}$=	0.815	1.300

		23.825×10^{12}		
Nitrogen (N_2)	~2.7%	$0.027\times25\times10^{12}$= **$6.75\times10^{11}$**	1.040	1.404
Argon (Ar)	~1.6%	$0{,}016\times25\times10^{12}$= **$4\times10^{11}$**	0.524	1.667
Oxygen (O_2)	~0.17%	$0{,}0017\times25\times10^{12}$= **$4.25\times10^{10}$**	0.913	1.40

Thus Table 2 shows the proportion of main gases (useful to implement the proposed energy supply systems consisting of Power supplies based on SSPMs.

The adiabatic index shown in Table 2 for every potential working fluid is an essential characteristic of thermal working fluids, since exhibits a great influence on performance of every adiabatic heat-work interaction. In the same way, specific heat exerts a strong influence on the specific work of any heat-work interaction.

2.2 Essential resources for future human exploration

Apart from the gases available on the surface of Mars, which are useful for the implementation of energy supply services, there are also other very useful resources available to be exploited by humans. Therefore, Mars has a variety of resources that could be essential for future human exploration, colonization, and even in-situ resource utilization (ISRU). Next data illustrates a list of the main useful resources known or strongly suspected to exist on the Martian surface:

Water (H_2O) Ice: Found in polar ice caps (water and CO_2 ice) and subsurface glaciers.

Hydrated Minerals: Clays (e.g., smectite), sulfates (e.g., gypsum), and perchlorates.

Brine (Liquid Water): Possible seasonal seeps (recurring slope lines) - RSLs) and deep aquifers.

Carbon Dioxide (CO_2): Atmosphere: ~96% CO_2, which can be processed into oxygen (O_2) and carbon monoxide (CO) for fuel.

Dry Ice: Frozen CO_2 at the poles.

Oxygen (O_2): Extracted from CO_2 (via MOXIE-like technology) or from water electrolysis.

Regolith (Martian Soil): Silicates: For construction (bricks, glass, ceramics) via sintering or 3D printing.

Iron Oxides: Hematite (Fe_2O_3) and magnetite (Fe_3O_4) for steel production.

Perchlorates (ClO_4^-): Useful as an oxidizer in rocket fuel (but toxic to humans).

Metals & Minerals: Iron (Fe): Abundant in regolith as oxides.

Aluminum (Al): In plagioclase and other aluminosilicate minerals.

Magnesium (Mg) & Calcium (Ca): In basaltic rocks.

Sulfur (S): In sulfates, useful for concrete (Martian cement).

Silicon (Si): For solar panels and electronics.

Nitrogen (N_2): Trace amounts (~2.7%) in the atmosphere, crucial for agriculture (fertilizer) and breathable air mixes.

Methane (CH_4): Detected in trace amounts; could be synthesized via the Sabatier reaction according to the reaction balance: ($CO_2 + H_2 \rightarrow CH_4 + O_2$) for instance as propulsion fuel in take-off-based rocket operations.

Noble Gases: Argon (Ar): Present in the atmosphere (~1.6%), useful for industrial processes.

Rare Elements (Trace Amounts): Lithium (Li), Nickel (Ni), Zinc (Zn): Possibly present in certain mineral deposits.

Table 3 illustrate a summary of the activities that could be carried out in the development of resource exploitation on Mars.

Table 3: Potential Uses

Uses	Demanded materials	Importance
Life Support	Water, oxygen, nitrogen	high
Fuel Production	Methane, hydrogen, perchlorates	high
Construction	Regolith-based concrete, metals, glass.	high
Agriculture	Water, nitrogen, CO_2 for greenhouse farming	high
Mining	Mining of materials susceptible to use after their detection and exploitation in accordance with the development of autonomous mining activities on Mars	high

With respect to mining, special importance is paid to minerals such as iron and aluminum. In fact both iron and aluminum can be treated and processed using electric power.

Iron: A new electrochemical process has been developed to extract iron from iron oxide using electricity instead of traditional blast furnaces. This method involves passing electricity through liquid containing iron-rich materials, isolating the metal without the need for extreme heat. This process is cleaner and potentially more cost-effective, reducing emissions and improving energy efficiency.

Aluminum: Electric current can also be used in the processing of aluminum alloys. By applying an electric current during the solidification of aluminum alloys, researchers have observed significant changes in the microstructure of the metal. This method can refine the material's properties and improve its performance.

2.3 Available procedures to obtaining local resources on Mars atmosphere

The Martian atmosphere is composed primarily of carbon dioxide (CO_2, ~95%), with smaller amounts as shown in Table 1 of N_2, Ar, O_2, and CO. Therefore, separating these components is crucial for in-situ resource utilization (ISRU) to support human missions (e.g., producing oxygen for life support or indeed methane fuel). Below are key technologies for separating these gases:

2.3.1 Carbon Dioxide (CO_2) Separation

-- Solid Amine (SA) Adsorption (e.g., MOXIE on Perseverance rover). Uses amine-functionalized adsorbents to selectively capture CO_2 at low pressure.

-- Released when heated (~150°C).

-- Pressure Swing Adsorption (PSA)

-- Zeolites or activated carbon selectively adsorb CO_2 under pressure.

-- Cryogenic Freezing: CO_2 freezes at ~–125°C (Mars nighttime temperatures can reach –73°C, but colder conditions may be needed for efficient capture).

-- Electrochemical, that is Solid Oxide Electrolysis, (SOEC)

-- Mars Oxygen In-Situ Resource Utilization Experiment (MOXIE) uses solid oxide electrolysis to split CO_2 into O_2 and CO.

2.3.2 Nitrogen (N_2) and Argon (Ar) Separation

-- Membrane Separation: Polymer or ceramic membranes allow selective permeation of lighter gases (N_2, Ar) over CO_2.

-- Cryogenic Distillation: CO_2 liquefies first (~–78.5°C), leaving N_2 and Ar as gases.

-- Further cooling separates N_2 (bp: –195.8°C) from Ar (bp: –185.8°C).

-- Pressure Swing Adsorption (PSA) for N_2/Ar

-- Carbon molecular sieves can preferentially adsorb N_2 over Ar.

2.3.3 Oxygen (O_2) Extraction

-- Electrolysis of CO_2 (MOXIE-like systems)

-- Solid Oxide Electrolysis (SOEC): Splits $CO_2 \rightarrow CO + \frac{1}{2}O_2$.

-- Molten Carbonate Electrolysis: Alternative high-efficiency method.

-- Thermal Decomposition of Metal Oxides (Carbothermal Reduction)

-- Oxides like perovskites release O_2 when heated.

-- Plasma Pyrolysis (Non-thermal Plasma) breaks CO_2 into O_2 and CO without extreme heat.

2.3.4 Integrated Approaches for Mars ISRU:

-- First Step: CO_2 Capture (SA, PSA, or cryogenic).

-- CO_2 Processing: Electrolysis (MOXIE) or Sabatier reactor according to ($CO_2 + H_2 \rightarrow CH_4 + O_2$).

-- N_2/Ar Separation: Cryogenic or membrane-based methods for buffer gas (life support) or inert gas uses.

2.3.5 Strategies to obtain hydrogen

Electrolysis of Martian Brines:

Researchers at Washington University in St. Louis have developed a system that can produce ultrapure hydrogen and oxygen from liquid Martian brines at very low temperatures. This system uses a novel brine electrolyzer that incorporates a lead ruthenate pyrochlore anode and platinum on carbon cathode.

A Dissolved perchlorate salts in Martian water prevent freezing and improve the electrolyzer's performance by lowering electrical resistance.

In-Situ Resource Utilization (ISRU):

SpaceX and other space agencies are focusing on ISRU techniques to leverage Martian resources for sustaining human presence and enabling return missions. One approach involves extracting water ice from the Martian surface, which can then be split into hydrogen and oxygen through electrolysis

B This method is crucial for reducing payload mass and increasing mission sustainability.

Mars Aromatic Hydrocarbon and Olefin Synthesis System (MAHOSS):

Pioneer Astronautics has developed the MAHOSS method, which produces storable low hydrogen/carbon ratio fuel and oxygen on Mars. This system utilizes 98% of the required raw material mass derived from the Martian atmosphere

C . This approach focuses on synthesizing hydrocarbons and olefins, which can be used as fuel.

These strategies highlight the importance of utilizing Martian resources to produce hydrogen, which is essential for fuel and life support systems. Each method leverages different aspects of the Martian environment, from brine electrolysis to atmospheric synthesis, to achieve efficient hydrogen production.

Main challenges:

-- Low atmospheric pressure (~0.6 kPa vs Earth's 101 kPa) necessitates compression.

-- Energy requirements (electrolysis, cryogenics) must be optimized for solar/nuclear power.

-- Dust contamination may affect adsorbents/membranes.

2.4 Minimum energy demand for sustained exploitation of a limited habitat on Mars

Estimating the electric energy consumption for separating the components of Mars' atmosphere (CO_2, N_2, Ar, O_2) depends on the technology used. Below is a breakdown of energy requirements for key processes, along with comparisons to Earth-based systems where applicable.

2.4.1 Carbon Dioxide (CO_2) Capture & Separation

Given the abundance of carbon dioxide in the Martian atmosphere, it is of paramount importance to harness it for as many applications as necessary. Given the abundance of carbon dioxide in the Martian atmosphere, it is of paramount importance to harness it for as many applications as necessary. Table 4 shows a summary of the applications and extraction and processing methods, as well as the electrical power requirements for such tasks on an industrial scale.

Table 4: Illustration of several metods to capture and separate CO2 associated with energy demand

Method	Energy Consumption	Comments
Solid Amine Adsorption (e.g., MOXIE)	~300–500 Wh/kg CO_2	Includes heating for regeneration (~150°C).
Pressure Swing Adsorption (PSA)	~200–400 Wh/kg CO_2	Depends on compression needs (Mars' low pressure requires pre-compression).
Cryogenic Freezing	~500–800 Wh/kg CO_2	High due to cooling to –125°C (Mars' cold nights help, but active refrigeration is needed).
Electrolysis (MOXIE-style SOEC)	~600–1000 Wh/kg O_2 (~2000–3000 Wh/kg CO_2 processed)	Splits $CO_2 \rightarrow CO + ½O_2$; efficiency ~30–50%.

Key considerations for Mars include at least the following power consumers:

Compression penalty: Mars' atmosphere is ~0.6 kPa (vs Earth's 101 kPa), so ~10–20% additional energy is needed for gas intake.

Thermal management: Heating/cooling systems add parasitic loads (radiators, insulation).

2.4.2. Nitrogen (N_2) & Argon (Ar) Separation

Table 5 includes a summary of the main energy consumers associated with separation tasks performed in the Martian atmosphere. Given the restrictive conditions of the Martian surface, in-situ energy production constitutes a significant contribution to the industrialization of the Martian surface. Autonomous, local, and intensive energy generation using sufficiently robust engines constitutes the basis for the industrialization of Martian industrial processes.

Table 5: Summary of energy costs to produce N_2 and Ar

Method	Energy Consumption	Comments
Cryogenic Distillation	~1000–1500 Wh/kg N_2/Ar	Requires cooling to –195°C (N_2) and –185°C (Ar).
Membrane Separation	~300–600 Wh/kg N_2/Ar	Lower energy but less pure output; may require multiple stages.
PSA for N_2/Ar	~400–800 Wh/kg N_2	Carbon molecular sieves preferentially adsorb N_2.

Key Challenges

Low N_2/Ar concentration (combined ~4.7%) means processing ~20–25 kg of Martian atmosphere per kg of N_2/Ar.

Cryogenics are energy-intensive but may be necessary for high-purity buffer gases (e.g., for habitats).

2.4.3. Oxygen (O_2) Production

Creating a breathable atmosphere requires large amounts of oxygen and nitrogen, as well as production tools compatible with the raw materials being processed. Thus Table 6 shows the demand of electric power to obtain oxygen.

Table 6: Summary of energy costs to produce O_2

Method	Energy Consumption	Comments
CO_2 Electrolysis (SOEC)	~3000–4000 Wh/kg O_2	MOXIE operates at ~3000 Wh/kg O_2 (~30% efficiency).
Molten Carbonate Electrolysis	~2500–3500 Wh/kg O_2	Higher efficiency than SOEC but more complex.
Thermal Decomposition (Perovskites)	~4000–6000 Wh/kg O_2	Requires high temperatures (~800–1000°C).

Key Considerations

-- MOXIE's baseline: Produces 6–10 g O_2/hour using ~300 W (~30,000 Wh/kg O_2, but real-world systems can be optimized to ~3000 Wh/kg).

-- Sabatier reactors ($CO_2 + H_2 \rightarrow CH_4 + O_2$) can reduce net energy if H_2 is available (~1000–2000 Wh/kg O_2 equivalent).

2.4.4 Total Estimated Energy for a Mars ISRU Plant

To produce 1 kg of O_2 and 0.5 kg of N_2/Ar buffer gas, the approximate energy budget as depicted in Table 7.

Table 7: Approximate energy demand to produce 1 kg of O_2 and 0.5 kg of N_2/Ar buffer gas

CO_2 Capture (1.5 kg processed):	Solid Amine/PSA:	~450–750 Wh
Cryogenic:		~750–1200 Wh
O_2 Production (1 kg): Electrolysis (SOEC):		~3000–4000 Wh
N_2/Ar Separation (0.5 kg): Cryogenic:		~500–750 Wh
Membrane/PSA:		~200–400 Wh
Total (optimized case):		~4000–6000 Wh per kg O_2 + buffer gas.

Power Supply Implications

A 1 kW solar array on Mars (assuming ~4–6 kWh/day after dust and daylight constraints) could produce ~0.7–1.2 kg O_2/day.

Nuclear (e.g., Kilopower 10 kW): Could support ~10–20 kg O_2/day, enough for a small crew.

Key Takeaways

CO_2 capture is the least energy-intensive step (~300–800 Wh/kg).

O_2 production dominates energy use (~3000–4000 Wh/kg).

N_2/Ar separation adds ~20–30% overhead if high purity is needed.

Conventionally, solar power is feasible for small-scale ISRU, but nuclear or advanced solar is needed for large-scale fuel/air production.

However, SSPMs are proposed because, in addition to providing unlimited power in intensity and time, they have enormous advantages over traditional techniques.

2.5 On the harvest of plants to produce oxygen and carbon dioxide on Mars

Harvesting plants on Mars to produce oxygen and carbon dioxide (CO_2) will be a crucial part of sustaining human colonies and regulating the atmosphere. Here's how it can be done effectively:

2.5.1 Selecting the Right Plants

Fast-growing, high-oxygen producers: Plants like heat, lettuce, spinach, and algae such as Chlorella or Spirulina) are efficient at photosynthesis and oxygen production.

C4 Plants: Some plants (like corn and sugarcane) use C4 photosynthesis, which is more efficient in low-CO_2 environments.

Cyanobacteria (Blue-Green Algae): These can be grown in water tanks and produce oxygen while also fixing nitrogen.

2.5.2 Controlled Environment Agriculture

Pressurized Greenhouses: Mars' thin atmosphere (95% CO_2 but at low pressure) requires sealed, pressurized domes or underground farms.

LED Grow Lights: Since sunlight on Mars is weaker (~43% of Earth's), artificial lighting tuned to photosynthetic wavelengths (red & blue) will be essential.

Hydroponics/Aeroponics: Soil-free farming saves water and allows precise nutrient control.

Temperature & Humidity Control: Mars averages -60°C, so heating and moisture retention systems are necessary.

2.5.3 Carbon Dioxide Management

Direct Use of Martian CO_2: The Martian atmosphere is 95% CO_2, which can be pumped into greenhouses to boost plant growth.

CO_2 Recycling: Human and plant respiration will naturally cycle CO_2 and O_2 in a closed-loop system.

Biochar Production: Burning excess plant matter in low-oxygen conditions creates biochar (carbon-rich material), which can store carbon and improve soil.

2.5.4 Oxygen Harvesting

Photosynthetic Oxygen Release: Plants release O_2 during photosynthesis, which can be captured and stored for human use.

Electrolysis Backup: If plants alone can't meet demand, electrolysis (splitting water into O_2 and H_2) can supplement oxygen production.

Algae Bioreactors: Microalgae can produce more oxygen per unit area than many plants and can be grown in compact systems.

2.5.5 Harvesting and Processing

Continuous Harvesting: Plants like algae and fast-growing greens can be harvested in cycles to maintain steady oxygen output.

Waste Biomass Utilization: Inedible plant matter can be composted or gasified to release CO_2 back into the system.

Genetic Engineering: Future crops could be optimized for Mars' conditions—higher radiation resistance, faster growth, and better gas exchange.

Challenges & Solutions

Low Atmospheric Pressure: Requires robust greenhouse structures.

Toxic Perchlorates in Martian Soil: Must be removed or avoided by using hydroponics.

Limited Water: Ice mining and water recycling will be essential.

Conclusion

By combining controlled agriculture, Martian CO_2 utilization, and efficient oxygen harvesting, plants can play a key role in making Mars habitable. Over time, large-scale bioregenerative life support systems could help terraform Mars by gradually increasing oxygen levels while managing CO_2 for plant growth.

2.6 Protections against UV and cosmic rays

With energy, robust shielding against UV radiation and cosmic rays on Mars is achievable using a combination of passive (physical) shielding and active (electromagnetic) shielding. Let s revise how can be done:

2.6. 1. Passive Shielding (Physical Barriers)

These are the most reliable methods and can be enhanced with sufficient energy for construction and maintenance.

A Thick Regolith (Martian Soil) Covering

Underground Habitats: Burying habitats under 2–3 meters of regolith blocks ~90% of cosmic rays and most UV.

Regolith Bricks/Concrete: Using sintered or compressed Martian soil to build protective structures.

Ice-Shielding: Water is an excellent radiation absorber—ice or water-filled walls add protection.

B Structural Shielding Materials

Polyethylene or Boron-Enhanced Plastics: Lightweight, hydrogen-rich materials that effectively block neutrons and secondary radiation.

Lead or Tungsten Layers: For high-energy cosmic rays, dense metals can be used in critical areas (but are heavy).

2.6. 2 Active Shielding (Electromagnetic & Energy-Dependent)

These require substantial energy but could supplement passive shielding.

A Electromagnetic Deflectors (For Charged Particles)

Superconducting Magnetic Shields:

A dipole or toroidal magnetic field (like a mini-magnetosphere) could deflect charged cosmic rays.

Requires high-temperature superconductors and megawatts of power (feasible with nuclear/fusion reactors).

Plasma Shields:

Ionized gas (plasma) could generate a protective bubble, but this is still theoretical.

B Atmospheric Enhancement (Long-Term Terraforming)

Artificial Greenhouse Gases: Releasing CFCs or perfluorocarbons could thicken the atmosphere, increasing natural shielding over centuries.

Ozone Layer Creation: If Mars regains a magnetic field, UV-blocking ozone could form.

C Active UV Filters

UV-Reflective Coatings: Thin metallic films on windows or domes can reflect harmful UV.

Electro-chromic Glass: Smart glass that darkens when UV levels are high (powered by solar energy/SSPM).

2.6. 3. Energy Requirements & Feasibility

The estimation of the electric power demand to keep a safe protection against cosmic ans solar radiation is depicted in Table 8.

Table 8: Illustration of the power demands to ensure radiation protection for common activities on Mars surface.

Shielding Method	**Power Needed**	**Feasibility on Mars**
Underground habitats	Low (excavation)	Easiest, near-term
Magnetic deflector	10–100 MW	Needs advanced reactors or **SSPMs**
Plasma shield	1–10 MW	Highly experimental: needs **SSPMs**
Regolith sintering (construction)	High thermal energy demand	Possible with nuclear/solar/SSPM

Best Power Sources:

Traditional technologies: Nuclear (Kilopower, Fission Reactors) → Best for high-energy needs.

Solar (With Energy Storage) → Limited but useful for UV filters.

Future Fusion Reactors→ Ideal for large-scale active shielding.

Proposed Power Sources: **SSPMs** and **CCs** based on the combination of **(RBC-SSPMs)**

Conclusion

Short-Term (Next 50 Years): Underground habitats + regolith shielding will dominate.

Mid-Term (Next 100 Years): superconducting magnetic shields could protect surface cities if energy is abundant.

Long-Term (Terraforming): A restored magnetic field + thicker atmosphere would make passive shielding enough

2.7 Details on NASA or SpaceX's proposed radiation shielding tech

Both NASA and SpaceX have explored (or are developing) advanced radiation shielding technologies for Mars missions and habitats. Here's a detailed breakdown of their approaches [5-7]:

NASA's Radiation Shielding Technologies

NASA has been researching Martian radiation protection for decades, focusing on passive shielding, magnetic deflectors, and material science.

A Passive Shielding: Regolith & Habitats

Mars Ice Home (2016). A proposed inflatable habitat covered in a layer of ice (water is an excellent radiation shield).

Uses Martian water ice to block cosmic rays while allowing natural light.

Power Needs: Minimal (just thermal regulation).

Regolith Sintering (RAMs, 2020s)

NASA's Selective Laser Sintering (SLS) experiments aim to 3D-print structures from Martian soil.

Kilopower nuclear reactors could provide energy for sintering.

B Active Shielding: Magnetic Deflectors

Magnetic Radiation Shield (2017, NASA NIAC Study)

A mini-magnetosphere (like Earth's) to deflect charged particles.

Requires superconducting coils ~10 Tesla field) and ~10 MW of power (feasible with compact fusion or fission reactors).

Status: Concept study (no flight tests yet).

C Wearable & Vehicle Shielding

HERA & Orion Capsule Shielding

Uses polyethylene (hydrogen-rich plastic) to block neutrons.

Spacecraft walls may incorporate boron- or lithium-doped materials for better protection.

SpaceX's Approach (Starship & Mars Base)

SpaceX's strategy leans more toward rapid deployment using existing materials rather than futuristic active shielding (for now).

A Starship's Radiation Mitigation

Short Transit Time (~6 months) reduces exposure, but shielding is still needed.

Proposed Solutions:

Fuel & Water Walls: Storing fuel or water around crew areas for passive shielding.

Stainless Steel Hull: Thicker metal provides some protection but not enough alone.

B Mars Surface: Underground & Regolith Shielding

Elon Musk's Vision: Early Mars bases will likely be buried or covered in regolith.

3D-Printed Structures (Similar to NASA's approach, but using SpaceX's autonomous construction bots).

Transparent Domes (Long-Term): If radiation is mitigated, pressurized domes with UV-filtering glass could be used.

C SpaceX's Power Solution: Solar + Nuclear?

Solar Arrays: Likely initial power source, but limited by dust storms.

Possible Future Nuclear: Musk has hinted at small fission reactors (similar to NASA's Kilopower) for high-energy needs.

Comparative Summary: NASA vs. SpaceX

Table 9 illustrates the comparative approaches between radiation protection technologies proposed by NASA and SpaceX

Table 9: Comparative summary of radiation protection technologies approached by NASA and SpaceX

Technology	**NASA's Approach**	**SpaceX's Approach**
Passive Shielding	Ice homes, regolith sintering, polyethylene	Buried habitats, Starship water shielding
Active Shielding	Superconducting magnets (long-term)	Not a priority yet
Power Source	Kilopower nuclear reactors	Solar, possibly small nuclear later
Construction	3D-printed regolith structures	Autonomous bots + prefab units

Future & Experimental Concepts

NASA's Psyche Mission (2023): Testing deep-space radiation effects—data will help refine shielding.

MIT's Plasma Shield (2022): A "radiation bubble" concept, but needs ~1 MW of power.

ESA's Moon/Mars Village: Testing lunar regolith shielding as a Mars analog.

Conclusion:

Near-Term vs. Long-Term

2020s–2030s: NASA & SpaceX will rely on underground habitats, regolith, and water shielding.

2040s+: If compact fusion or advanced superconductors emerge, active magnetic shielding could revolutionize surface living.

Long-Term vs. SSPMs (available now)

By using the disruptive SSPMs, electric and/or mechanical energy can be utilized without the limitations of conventional power sources. These technologies can be used not only in plants but also in the cosmos of the local solar system.

This involves optimizing resources, which requires including technologies to implement underground plantations equipped with artificial light and sufficient, self-sustaining, and robust power supply on demand, in addition to all the necessary additives to harvest food and harness oxygen to generate new, useful atmosphere. Protection or insulation against ionizing radiation would not be necessary in underground environments, which represents significant energy savings. Backhoes and tunnel boring machines powered by attached SSPMs solve the problem of creating large underground plantations. Most crucial action to be considered is the ability to drill both to obtain mineral samples as well as to extract minerals for useful industrial applications and/or water to sustain plant and animal life in places located far from the poles where water is scarce, or do not exist near surface levels.

Therefore, next section deals with the task of developing and implementing prototypes of SSPMs enabled to operate with thermal working fluids extracted from the mars atmosphere. Furthermore, some technologies developed to transform Mars in terms of energy supply are versatile in terms of exploiting the solar system's resources. Moreover, being independent of solar and/or stellar energy opens the way to the autonomous exploration of other extra solar or cosmic systems.

3 Development and implementation of SSPMs-based prototypes capable of operating with TWF obtained from Martian atmosphere components

This section focuses on developing **Self Sustaining Powered Machines (SSPMs)** [10-18] designed to operate on the surface of **Mars**. Given the planet's unique conditions, these systems must be specially engineered not only to function in the Martian environment but also to utilize locally available resources.

The most critical resources for these SSPMs are those related to **energy supply**. Thus, this section prioritizes the development of **prototypes for disruptive power supply engines**.

Table 10 outlines the potential **Thermal Working Fluids (TWFs)** present in the Martian atmosphere. As such, SSPM prototypes must be capable of utilizing the gases listed in this table. The case studies presented here compare the performance of each gas as a viable TWF.

The table highlights the primary gases suitable for implementing the proposed **energy supply systems**, which consist of **cascaded Power Units (PUs)** and **Radioactive Balance Converters (RBCs)** in cases involving self-contained heat sinks. Based on availability and suitability, **argon and nitrogen** emerge as the best candidates. However, aside from argon, the TWFs found in Mars' atmosphere are unsuitable for RBCs if a **Combined Cycle (CC)** system is intended.

Table 10: Characteristics of TWFs obtained from the Martian atmosphere, useful for operating SSPMs in Martian industrial operations.

Gas names	Cp (kJ/kg K)	γ=Cp/Cv	Suitability of each TWF
Carbon dioxide (CO_2)	0.815	1.300	Low efficiency due to a low adiabatic index, Low specific work due to low specific heat
Nitrogen (N_2)	1.040	1.404	Acceptable for SSPMs
Argon (Ar)	0.524	1.667	Useful for SSPMs and RBCs. Highly efficient, despite providing low specific work.
Oxygen (O_2)	0.913	1.400	Similar to N2, but more corrosive
Synthetic Air (SA)	1.050	1.400	Acceptable for SSPMs.

The basic criteria for selecting TWFs are in-situ availability, physical and chemical stability, resistance to reactions with metals, heat capacity responsible for influencing specific work, and the adiabatic index responsible for influencing thermal efficiency. Therefore, Table 10 shows that argon and nitrogen are the most suitable TWFs.

3.1 Thermodynamic processes in cycles doing work by expansion and contraction heat-work interactions

The schemes depicted in Fig. 1 deals with the behavior of thermal cycles conducted by closed processes-base3d heat-work interactions. The particularly disruptive feature added is the concept of useful work performed by the thermal contraction of the TWF, exerted within the thermal cycle driving an actuator in question (**the work performed by contraction is due to cooling, and the unique output useful forces generated are pull or tensile forces**). Modeling cycles involving mechanical work due to expansion and contraction, as well as the adjustment of energy balances, do not fully comply with the FLT, so special treatment is applied. Eq. (1) and (2) show the differences between cycles that operate by expansion and cycles that operate by expansion and contraction forces by means of its respective energy balances.

In previous research works references [10-16], it has been demonstrated that low-grade heat can be efficiently converted to high-grade heat. This high-grade heat can then be supplied to the system. Achieving this requires a heat manipulation strategy involving a series of successive conversions with high efficiencies: low-grade heat to mechanical work, mechanical work to electrical power, and electrical power to high-grade heat. This can be carried out by PUs connected in cascade

Since this chaining of conversion stages involves inherent thermal losses, fortunately, applying an appropriate strategy based on upstream cascade heat recovery increases the degree of recovered heat, converting it into useful high-grade heat that can be added to the first power unit (PU) of a PU cascade. A necessary and sufficient condition for using a cascade of PUs capable of recovering and converting low-grade heat into high-grade heat is to use PUs capable of performing contraction work (i.e., work performed by means of tensile forces). Such forces can only be generated by generating a vacuum relative to a reference pressure by cooling based on heat extraction relative to a reference pressure of the thermal cycle.

Therefore, the basic characteristic that must meet every PU deals with its ability to perform useful mechanical work by contraction of the TWF, which give rise to a **pull force** achieved by extracting heat from the TWF instead of adding heat.

Let's begin by the energy balance for the case of a closed processes-based cycle that is enabled to operate by doing useful mechanical work by expansion

$$
\begin{aligned}
&q_{i12} - q_{o31} = w_n = w_{o23} \\
&w_{o\exp} = w_{o23} = \Delta u_{23} \\
&w_n = \sum w_o - \sum w_i = w_{o\exp} = w_{o23} \\
&\eta_{th} = \frac{w_n}{q_{i12}} = \frac{\Delta u_{23}}{q_{i12}}
\end{aligned}
\qquad (1)
$$

Equation (1) illustrates the energy balance of the Vsp (isochoric-adiabatic-isobaric) cycle, characterized by useful mechanical work through expansion, in which the first law of thermodynamics (FLT), (i.e., the principle of conservation of energy), is fulfilled.

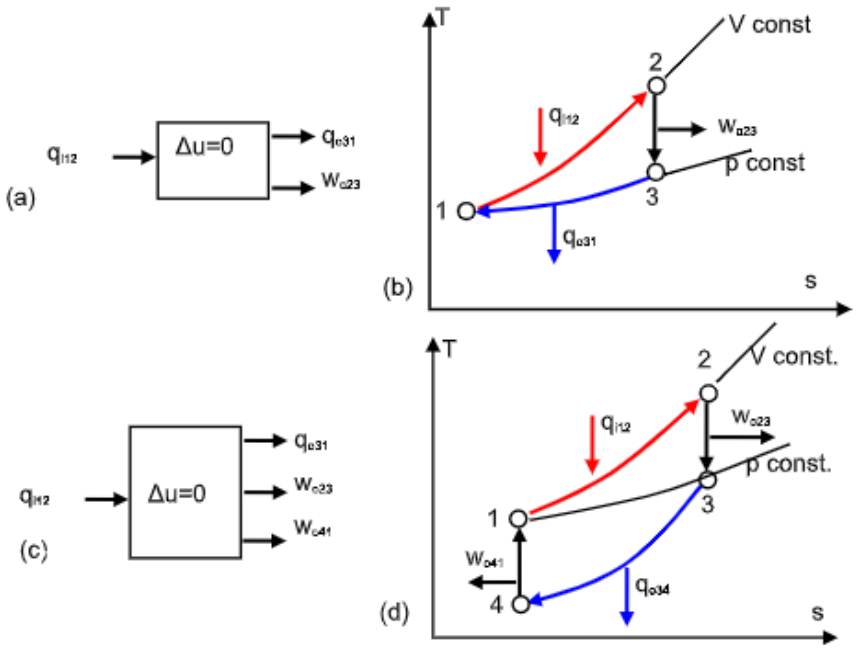

Figure 1: Closed processes-based cycles. (a): Block diagrams of the heat-work interactions during the cycle Vsp. (b): T-s diagram of the cycle **Vsp** doing work by expansion. (c): Block diagrams of the heat-work interactions during the cycle **VsVs**. (d): T-s diagram of the cycle VsVs doing work by expansion and contraction.

Now, let's consider the case of a thermal cycle based on closed VsVs processes, characterized by performing useful mechanical work through expansion and contraction. This means that it operates with both pushing and pulling forces. From its energy balance, it can be observed that the FLT is not fulfilled due to pulling forces.

$$
\begin{aligned}
&q_{i12} - q_{o41} \neq w_n \\
&w_{o\exp} = w_{o23} = \Delta u_{23} \\
&w_{ocont} = w_{o41} = \Delta u_{41} \\
&w_n = \sum w_o - \sum w_i = w_{o\exp} + w_{ocont} = w_{o23} + w_{o41} \\
&\eta_{th} = \frac{w_n}{q_{i12}} = \frac{w_{o23} + w_{o41}}{q_{i12}} = \frac{\Delta u_{23} + \Delta u_{41}}{q_{i12}}
\end{aligned}
\qquad (2)
$$

2.1.1 Comparison of consequences derived from Eq. (1) and (2)

Let us perform a simple analysis of the thermodynamic consequences in cycles involving forces originating from thermal contraction obtained by heat extraction [10-18]:

From equations (1) and (2) we deduce that:

in Eq. (1), $w_n = \sum w_o - \sum w_i = w_{o\exp} = w_{o23}$ which is different from

$w_n = \sum w_o - \sum w_i = w_{o\exp} + w_{ocont} = w_{o23} + w_{o41}$ depicted in Eq. (2),

while the input added heat to the cycle is the same, so that the energy balance in Eq. (2) is not consistent with respect to the energy balance of Eq. (1). Clearly the energy balance given by Eq.(2) needs a different treatment. Equation (2) illustrates the energy balance of the VsVs —isochoric-adiabatic-isochoric-adiabatic— cycle, characterized by doing useful mechanical work through expansion and contraction —**pull forces**—, in which the FLT is violated, i.e., the principle of conservation of energy is violated. This is because in Eq. (1) the general energy balances –FLT– is fulfilled according to the following energy balance:

$$q_i - q_o = w_o \rightarrow q_{i12} - q_{o31} = w_{o23} = w_{o\exp} \quad (3)$$

while in Eq. (2) the general energy balance –FLT– is not fulfilled according to the following energy balance:

$w_o \neq q_i - q_o$, since $w_o = w_{o\exp} + w_{ocont} \rightarrow q_i - q_o \neq w_{o\exp} + w_{ocont}$, (4)

That is: the output useful **pull force** which gives rise to the useful contraction work —w_{ocont}— contributes to increase internal energy along the contraction process of the cycle, which is not consistent with the energy balances that exhibit only **push forces**, that is expansion work. Both aspects are illustrated in the Fig. 1 by means of its block diagrams of energy balances and its T-s diagrams.

Finally, according to irrefutable arguments based on equations (3) and (4), the inconsistency of energy balances including traction forces with respect to those including only thrust forces justifies considering the extension of energy balances based on the first law to take into account heat-work interactions affected by traction forces.

In conclusion, traditional thermal cycle energy balances only consider the energy input (qi + wi) and the energy output (q_o + w_o), i.e., (q_i + w_i) = (q_o + w_o), since the internal energy does not vary throughout a cycle. However, although this statement is absolutely rigorously true and therefore irrefutable, it does not hold true if, and only if, heat-work interactions, including pull or attractive forces, exist. This is because heat extraction (energy output) contributes to useful work output, which upsets the traditional energy balance.

Even if we consider the energy balance based on thermal cycles that only use heat-work interactions based on the performance of useful work through expansion, we can observe inconsistencies with the principle of conservation of energy that we can summarize in the following subsection.

2.1.2 Energy balance of a closed process-based cycle, including only expansion work.

Referring to Fig. 1(b), the cycle includes three heat-work interactions based on closed processes:

1-2: isochoric heat addition qi, 2-3: adiabatic-isentropic outflow expansion work w_o, and 3-1: isobaric heat rejection q_o. The corresponding energy balance is completed with: q_i,— q_o — w_o = 0, or: q_i,— q_o = w_o, since in a cycle based on closed processes, the changes in internal energy are zero.

If we consider a successive sequence of cascading energy conversion cycles, following the cycle represented in Fig. 1(b), it is observed that only a fraction of the total energy (heat-work) added to the cycle is converted into mechanical work, while the remaining heat rejected by the current conversion cycle is sent to the next. If the same conversion cycle is repeated indefinitely, it is observed that the total heat rejected in the infinite steps of the conversion process is equal to the heat added at the beginning (the first cycle executed). This means that the energy (heat-useful work) has been completely dissipated and, therefore, has not been conserved and is therefore not susceptible to utilization. The capacity to perform work has been nullified.

Figure 2(b) illustrates how a sequence of successive executions of a thermal cycle, starting from an initial amount of heat (Ei = qi), is converted into both output useful work (w_o) and heat rejected (q_o), where the heat rejected in each cycle has been reused as input energy for the execution of the next cycle. According to the results, as the sequence of conversion steps approaches infinity, w_o and q_o approach zero.

According to Fig. 2, as the heat rejected in each conversion cycle approaches zero, the total value of heat rejected reaches a value equal to that of the initial input energy. That is, the input heat has been used both in rejection and in the production of useful work, only to be reincorporated into the next conversion cycle, until it loses its ability to perform dynamic physical changes or produce useful work.

Experimental observation suggests that from a potential difference between two states of a physical magnitude, nature inherently tends towards equilibrium, where in each case of a causal system, if and only if there are no external forces that destabilize the system such as external excitations and disturbances, it tends towards

equilibrium, which means that its capacity to produce changes has been annulled and therefore its capacity to perform work.

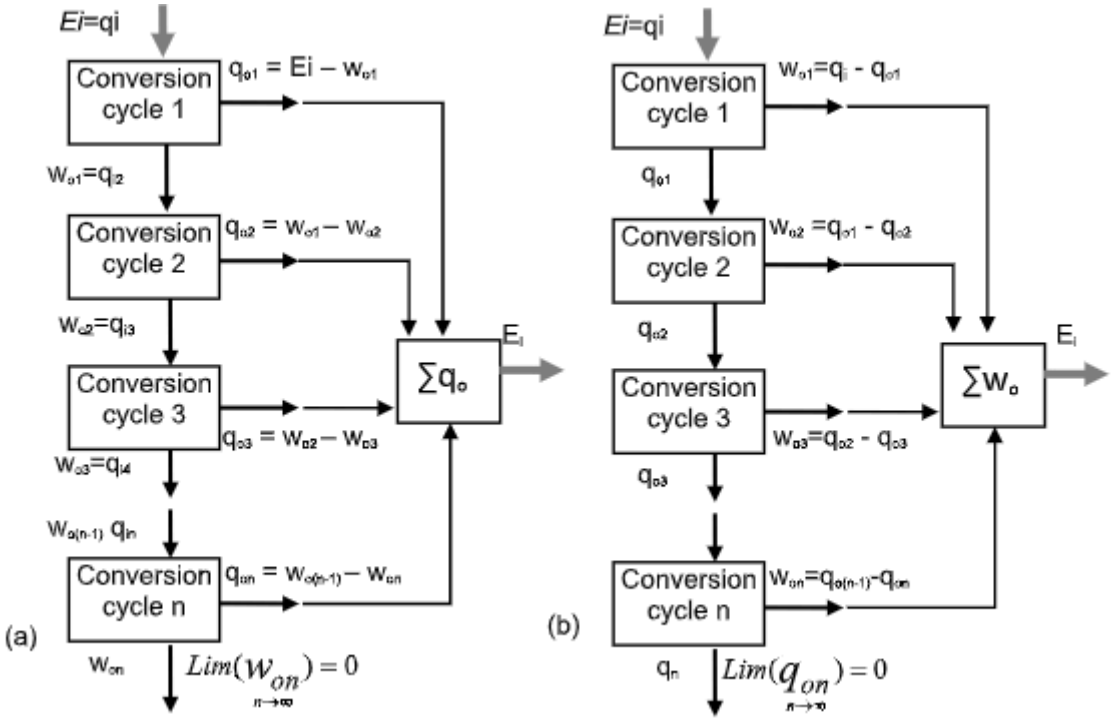

Figure 2: Consistence of the energy balance of thermal cycles based on the FLT by means of a sequential procedure of energy conversion cycles in a closed processes-based thermal cycle obeying the energy balance given by FLT depicted in Eq. (1)

In Fig. 2(a) it is shown that while the output useful work is zero, the rejected heat equals the input added energy, verifying energy conservation. Eq. (5) and (6) shows the above commented case by following the block diagram of Fig. 2(a).

Thus the total rejected heat in infinite conversion steps or repeated cycles is

$$q_{oTOTAL} = \sum_{1}^{n} q_o = [E_i - w_{o1}] + [w_{o1} - w_{o2}] + \\ + [w_{o2} - w_{o3}] + [w_{o(n-1)} - w_{on}] = [E_i - w_{on}] = E_i = \\ [E_i - q_{i2}] + [w_{o1} - 1_{i3}] + [w_{o2} - q_{i34}] + [w_{o(n-1)} - q_{in}] = \\ = [q_i - w_{on}] = q_i \quad (5)$$

Os simplifying, results in

$$q_{oTOTAL} = \sum_{1}^{\infty} q_o = E_i = q_i \quad (6)$$

The result of Eq. (6) is achieved from the limit depicted in Eq. (7)

$$q_{oTOTAL} = Lim \sum_{n=1}^{n=\infty} q_o = Lim_{n\to\infty}(E_i - w_{on}) = Lim_{n\to\infty}(E_i - 0) = E_i \quad (7)$$

Finally, taking limits on the infinite sequence of output works according to Eq. (8) follows that

$$Lim_{n\to\infty}(w_{on}) = 0 \quad (8)$$

In Eq. (8) it is verified that no useful work is done, so that the total input at high-grade energy is converted into low-grade heat or not useful heat, although it is conserved on the basis of the FLT-based energy balance.

Following the Block diagram of Fig 2(b) the total output work in infinite conversion steps or infinite repeated cycles is :

$$W_{oTOTAL} = w_{o1} + w_{o2} + w_{o3} + \cdots + w_{on} =$$
$$[q_{i0} - q_{o1}] + [q_{i0} - q_{o2}] + [q_{o2} - q_{o3}] + [q_{o3} - q_{o4}] + \cdots + [q_{o4} - q_{o(n+1)}] =$$
$$\sum_{1}^{n} [q_{i0} - q_{on}] \tag{9}$$

which yields

$$W_{oTOTAL} = \sum_{1}^{n} [q_{i0} - q_{on}] = Lim \sum_{n\to\infty}^{\infty} [q_{i0} - q_{on}] = q_{i0} - 0 = q_{i0} \tag{10}$$

In both sequences of successive conversion processes depicted in Fig. 2(a) and Fig. 2(b), the input energy is transformed from the heat state to the work state and rejected heat. Depending on the balance considered, if the total work obtained by converting heat to work —case (a) — is considered, then the heat rejected is zero because all the input heat has been converted into useful mechanical work, while if the heat rejected in each cycle of heat-to-work conversion is considered —case (b) —, then the work in the cycle n = infinity is zero because all the heat rejected corresponds to the input energy, and no useful work remains; that is, the capacity to perform useful work has been annihilated. In both cases energy has been conserved fulfilling FLT. However, If contraction-based work achieved by means of pull forces due to heat extraction, the above asseveration is not fulfilled, as shown in Eq. (2) or Eq.(4).

Key facts: The consequences of the inconsistence between Eq. (1) and Eq. (2) or Eq. (3) and (4) suggest us to include such heat-work interaction on an the extended FLT, in order to consider the observed real and irrefutable facts.

On the basis of the meaning derived from Eq. (2), as well as the significance of Fig. 2, the **energy balance** based on the FLT applied to thermal cycles that output useful mechanical work solely through expansion of the thermal working fluid, or that involve heat-work interactions based on expansion and/or compression, **is not applicable** to systems operating through thermal cycles that involve heat-work interactions enabled to do useful mechanical work by thermal contraction. Two main key facts are considered:

1 When thermal contraction is used for cooling through heat extraction, additional work is produced beyond the expansion work, which must be taken into account: **contraction work**.

2 The heat rejected by a thermal cycle operating by contraction and expansion can be recovered through regeneration with high efficiency and is therefore not rejected to the heat sink, so that it is not rejected heat.

Regarding conservation principles, these are rigorously supported by irrefutable theorems within the scope of the existence of ideal symmetric systems. Therefore, Noether's theorem is rigorously irrefutable, but not applicable to real systems. Real systems are characterized by a strong independence from the mathematical models that define them. That is, real systems do not obey the mathematical models generated from ideal systems. They exhibit inherent losses or irreversibilities that lead to the destruction or annihilation of useful energy and, after a cascading succession of heat-work interactions, are incapable of causing dynamic changes in real processes and, therefore, incapable of performing useful mechanical work. Useful is understood as capable of modifying something. Consequently, Noether's theorem is not applicable to real systems, but ideal systems which include full isolated systems.

2.1.3 Key consequences

The initial energy added is dissipated over the cycles of energy conversion to work, which means it has been annihilated and therefore not conserved. This non-recoverable or lost energy lacks the ability to be converted back into useful work or produce any dynamic physical change.

It must be recognized that if there is no potential difference between two states of a continuous function of any physical magnitude, energy is not possible, and therefore no useful mechanical work can be performed.

Without such a potential difference, there is no capacity to perform useful work. Without useful work, no dynamic change is possible because a unique and sufficient condition to provoke a change is mechanical work.

The fact that at stage n of a thermal cycle, whose input heat is the heat rejected in the previous conversion process, the energy is zero means that there is no longer any useful energy to convert, and therefore, its capacity to continue the conversion processes has been eliminated.

When the potential difference of a physical quantity is zero, a state of equilibrium is achieved, meaning that no dynamic change is possible without an external force on the system. Therefore, the concept of energy conservation following a succession of thermodynamic transformations leading to a state of equilibrium is untenable.

3 Empirical validations through case studies

Taking into account the considerations given in subsections 2.1.1 and 2.1.2 regarding the fulfillment of the energy conservation concepts associated with FLT, let us consider the implementation of the case study as two groups of power plant prototypes, since it involves studying two Power Plant (PP) structures that fulfill two different application demands, depending on the on-site or local environment:

1 Self-Sustaining Power Plant (SSPP) implemented by means of a group of cascaded of PUs characterized by its ability to operate without any external Power Supply (PS)

2 Combined-cycle structure consisting of a HP heat pump consisting of a Reverse Brayton Cycle (RBC) and a cascade of PUs that constitutes a SSPM. The RBC operates with Argon (Ar) as the TWF as illustrated by Table 11. The reason for using Ar as TWF instead of Nitrogen (N2), or Carbon Dioxide (CO2), abundant on Mars atmosphere is that the adiabatic expansion coefficient of mentioned TWFs except Ar is too low compared to that of Ar. The power units operate with N2, CO2, Air or Ar as the TWF.

Fig. 3 illustrates both mentioned concepts of SSPMs [10-16]. In Fig. 3(a) it is shown a SSPM composed by a group of cascaded PUs, while in Fig 3(b) a simplified coupling scheme of a heat pump formed by the RBC with the SSPM formed by a cascade of PUs. The design of the heat pump must satisfy the condition of supplying the heat demand of the first PU of the SSPM plant, as well as absorbing the heat rejected by the last power unit of the cascaded PUs of the SSPM plant.

Fig. 3(b) illustrates a RBC coupled to a SSPM to achieve the self heat source (SHS) and a self heat sink (SHSk) giving rise to a complete autonomous SSPM enabled to operate without any external power source and power sink, which defy some second law statements. In the concerned case study a reversed Brayton cycle (RBC) is combined with a cascade of PUs enabled to perform useful mechanical work under operational self-sufficiency. The function of the RBC is to perform the functions of a thermal energy supply source and a thermal energy sink source while the cascade of PUs is responsible for transforming the thermal energy into work and/or electrical power.

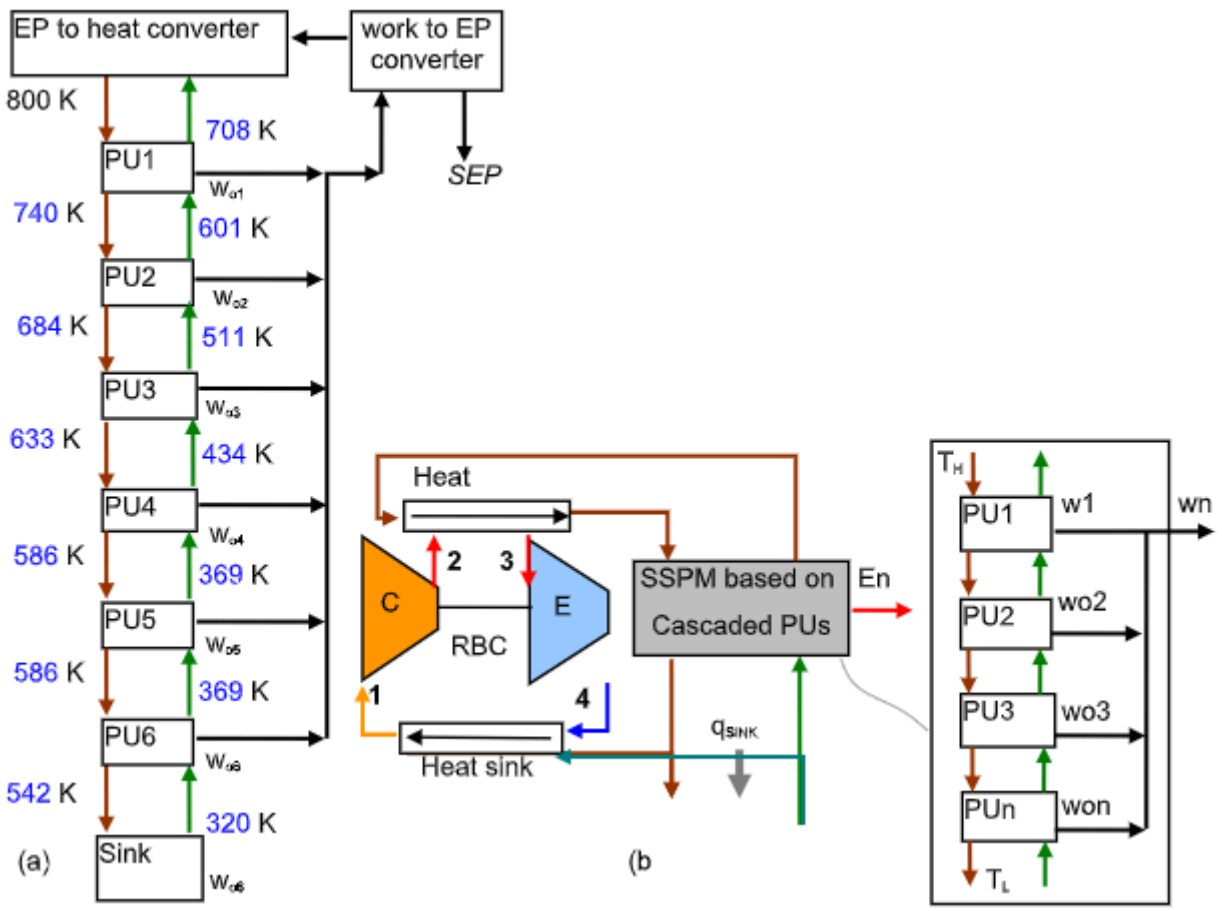

Figure 3: Schematic structure a CC composed by a SSPM coupled to the RBC [19-21]. (a) Depicts the HP based on a RBC. (b), illustrates the SSPM composed by a cascade of 6 PUs

3.1 Implementing Case Studies Aimed at Prototyping SSPMs and CCs Based on (RBC-SSPM)

The study of the different cycles concerns the local resources of thermal working fluids that either exist in the Martian atmosphere or can be obtained from it. Therefore, Table 11 illustrates the possible combinations of plant structures based on SPMs and TWFs compatible with such plant structures. Oxygen (O_2) will not be taken into consideration due to its high corrosive potential, since there are others with advantages in both abundance and extraction facilities, and ease of obtaining. According to the table data, Ar is applied to the RBS for any plant structure combination, while the SSPMs based on Cascaded PUs can operate with all available fluid. Furthermore, Table 11 shows two groups of PPs. The first belong to SSPMs that include TWFs such as argon, nitrogen, air, carbon dioxide, and oxygen, while the second belong to CCs that include argon-argon, argon-nitrogen, argon-air, argon-carbon dioxide, and argon-oxygen.

Table 11: Available TWFs and compatibility to be used on SSPMs based on a group of cascaded PUs and a CC-based (RBC-SSPM)

Available TWFs	TWF for SSPMs	TWF for RBC	TWFs for CCs based on RBC-SSPMs
Ar	Ar		Ar - Ar
N_2	N_2		Ar – N_2
Air (SA)	Air	Ar	Ar - SA
CO_2	CO_2		Ar - CO_2
O_2	O_2		Ar - O_2

Figure 4: Block diagrams of the energy flows. (a) illustrates a general scheme of SSPM with externaal heat sink. (b) illustrates a general scheme of CC based (RBC-SSPM)without externaal heat sink.

Fig. 4 illustrates the general echemes corresponding to the SSPM depicted in Fig. 4 (a) and the CC based on the combination of a RBC and a SSPM composed of a set of cascaded PUs depicted in Fig. 4 (b) similar to that of Fig. 4(a). If we consider the practical application site as Mars, the combined cycle option shown in Fig. 4(b) is not necessary since there is a natural heat sink in the Martian atmosphere due to its low mean temperature. Therefore, a SSPM is sufficient, simpler, less expensive, and easier to maintain.

3.2 Heat Pump as heat source and sink

The thermodynamic study of the heat pump based on a RBC is carried out using the data from [15] for Argon as real TWF. Therefore, Table 12 depicts the data corresponding to the open-process-based RBC responsible for performing the tasks of heat supply power source and heat sink, both operating as a heat pump with Argon as the TWF. The general structure of the heat pump-based RBS is represented in Fig 3(b).

The heat pump is implemented by means of a RBC responsible for supplying heat to the associated group of cascaded PUs and extract heat from the group of cascaded PUs that give rise t a SSPM. Thus, the sequence of open processes corresponds to the RBC structure depicted in Fig. 3(b). Used data has been taken from the database referenced as [ss]. The design criteria for both heat and cold sources are more in line with the need to satisfy the cold and heat demands to feed the PU cascade than to obtain a high COP value.

Table 13 illustrates the main RBC results operating as heat pump with Ar as TWF. The results derived from the heat pump implemented by means of a RBC operating under open system-based processes and computed with data from Table 12. Inlet compressor pressure p_1=1(bar); outlet compressor pressure p_2=1.55; compressor pressure ratio (PR)=1.55. Since the RBC is responsible for supplying the demanded amount of heat as well as the demanded amount of cold to ensure the isolated heat sink tasks, let's consider the relevance of the data shown in Table 13. Therefore in order to supply the necessary heat and dissipate the rejected heat to/from the SSPM consisting of a group of cascaded PUs, an energy balance of heat input and dissipation is carried out using a heat dissipation energy balance to obtain the flow rate of heat dissipation fluid through the RBC. This determines the RBC cycle stress so that it meets the heat sink demand. This results in excess high-grade thermal energy produced by the RBC compressor, which can be utilized both as direct heat and to power other devices, including another power plant. The methodology used to resolve the case studies has been described an applied in a previous work referenced as [18].

Table 12: Illustration of the RBC data corresponding to Ar as TWF enabled to operate as heat pump to provide a SHS for self input heat and a SHSk to absorb the heat rejected by the SSPM.

RB-Ar	T(K)	p(bar)	V(m^3/kg)	u(kJ/kg)	h(kJ/kg)	h'(kJ/kg)	s(kJ/kg-K)
1	680.00	1	1.4157	212.24	353.8	353.8	4.3051
2	810.00	1.5489	1.0889	252.81	429.0	421.5	4.3051
2a	690.00	1.5489	0.9276	215.33	359	359	4.2216
3	340.00	1.5489	0.4567	105.94	176.7	176.7	3.8529
4	286.00	1	0.5917	89.12	148.6	148.6	3.8529
4a	340.00	1	0.7075	106.01	176.75	176.75	3.9442

The RBC computed with the data from Table 12 is depicted in Table 13. The relevant data depicted in this table deals with the parameters that sustain the heat source and heat sink, that are: Available Self Heat Source (SHS) (kJ/kg) = **70** and Available Self Heat Sink (SHSk) (kJ/kg)= **28.2**, while the amount of work demanded by the heat pump, which must be ext5recyted from the SSPM, approaches 47.12 (kJ/kg).

Table 13: Depiction of the RBC results operating with **Ar** as TWF

Work done on the compressor of the RBC (kJ/kg)	W_{i12}= w_{i_comp} (kJ/kg)	75.19
Total pumped heat (kJ/kg)	q_{o23} (kJ/kg)	253.33
Work done on by the expander of the RBC (kJ/kg)	W_{o34} = w_{o_exp} (kJ/kg)	28.7
Total recovered heat to the compressor suction side (kJ/kg)	q_{i41} (kJ/kg)	14.79
Isentropic efficiency	Is_eff (%)	90
w_n (RBC)=w_{i_comp}-w_{o_exp}=q_i-q_o(kJ/kg)	RBC work demand (kJ/kg)	**-47.12**

Coefficient of performance for the RBC	COP	5.71
Available Self Heat Source (SHS) (kJ/kg)	Available SHS_(q_{o2-2a}) RBC(kJ/kg)	**70.0**
Available Self Heat Sink (SHSk) (kJ/kg)	Available SHSk_(q_{i4-4a}) RBC(kJ/kg)	**28.2**

Table 14 shows the heat flow ratios corresponding to SHSk and SHS formed by the RBC to extract and add the required heat from/to the cascade PU group. If the group of cascaded PUs that conforms the SSPM operates with **Ar** as TWF, then the second column of Table 14 shows the CCF and the HCF ration corresponding to **Ar**

Table 14: Illustration of the Cooling Capacity and Heating Capacity factors using **Ar** for both, the RBC-based heat pump and the group of cascade PUs

Cooling Capacity factor(CCF) (kJ/kg RBC)/(kJ/kg PU6) =	**1,81**
heating capacity factor(HCF) (kJ/kg)RBC/(kJ/kg PU1) =	**1,87**

3.3 Studying the SSPMs operated by the cycle VsVs in each group of six cascaded PUs

For prototyping PPs based on SSPMs, the following TWFs are used: argon, nitrogen, air, carbon dioxide.

For prototyping PPs based on CCc, the following TWF combinations are used: argon-argon.

The choice of only one CC is due to the high efficiency of Argon compared to the rest of the potential TWFs.

The cascaded PUs operating with a VsVs cycle responsible for converting the heat and cold obtained from the heat pump implemented by the RBC as available SHS and available SHSk are depicted in The ratio of cascaded temperatures (RIT) is selected as 0.85 for all TWF and the losses inherent to irreversibilities LS(%) and RF(%) are assumed 0.85 and 0,95 respectively. Table 15 a set of six cascaded PUs operating with **Ar** as TWF on the VsVs cycle is depicted.

Table 15 Illustration of the set of 6 PUs operating in cascade; table data corresponds to the real gas Argon as TWF. Values are taken from reference [NIST] for all considered gases

PU1-Ar	**T(K)**	**p(bar)**	**v(m^3/kg)**	**u(kJ/kg)**	**s(kJ/kg.K)**
1	680.00	10.000	0.14190	211.79	3.825
2	800.00	11.770	0.14190	249.29	3.876
3	750.00	10.000	0.15623	233.71	3.876
4	635.00	8.478	0.15623	197.78	3.825
PU2-Ar	**T(K)**	**p(bar)**	**v(m^3/kg)**	**u(kJ/kg)**	**s(kJ/kg.K)**
1	578.00	10	0.12058	179.82	3.740
2	680.00	11.7730	0.12058	211.71	3.791
3	637.00	10	0.13283	198.32	3.791
4	541.00	8.4920	0.13283	168.32	3.740
PU3-Ar	**T(K)**	**p(bar)**	**v(m^3/kg)**	**u(kJ/kg)**	**s(kJ/kg.K)**
1	491.30	10	0.10242	152.60	3.655
2	578.00	11.7770	0.10242	179.71	3.706
3	543.00	10	0.11236	168.84	3.706
4	462.00	8.5669	0.11236	143.51	3.655
PU4-Ar	**T(K)**	**p(bar)**	**v(m^3/kg)**	**u(kJ/kg)**	**s(kJ/kg.K)**
1	417.61	10	0.08695	129.41	3.570
	491.30	11.7830	0.08695	152.46	3.621
3	461.00	10	0.09566	143.07	3.621
4	398.70	8.6731	0.09566	123.58	3.570

PU5-Ar	**T(K)**	**p(bar)**	**v(m³/kg)**	**u(kJ/kg)**	**s(kJ/kg.K)**
1	354.96	10	0.07373	109.61	3.484
	417.61	11.7930	0.07373	129.23	3.535
3	392.00	10	0.08098	121.32	3.535
4	333.00	8.5348	0.08098	102.84	3.484
PU6-Ar	**T(K)**	**p(bar)**	**v(m³/kg)**	**u(kJ/kg)**	**s(kJ/kg.K)**
1	301.72	10	0.06244	92.69	3.398
	354.96	11.8050	0.06244	109.39	3.449
3	332.10	10	0.06885	102.36	3.449
4	282.50	8.4824	0.06885	86.79	3.398

Table 16 illustrates the results corresponding to a group of six cascaded PUs operated by a VsVs cycle with Argon as real TWF.

Table 16: Illustration of the results set of 6 PUs operating in cascade with real gas Argon as TWF depicted in Table 15

PU-Ar	1	2	3	4	5	6	total
LF(%)	0.85	0.85	0.85	0.85	0.85	0.85	0.85
RF(%)	0.95	0.95	0.95	0.95	0.95	0.95	0.95
RIT*100	85.0	85.0	85.0	85.0	85.00	85.0	85.00
T2(K)	800.00	680.00	578.00	491.30	417.61	354.96	
T1(K)	680.00	578.00	491.30	417.61	354.96	301.72	
qi_12/PU(kJ/kg)	37.50	31.89	27.11	23.05	19.62	16.70	155.87
qo_34(kJ/kg)	35.93	30.00	25.33	19.49	18.48	15.57	144.80
q_recov(kJ/kg)	34.13	28.50	24.06	18.52	17.56	14.79	137.56
Tm_qrecov(kJ/kg)		589.00	502.50	429.85	362.50	307.30	
wn(kJ/kg)	23.89	20.10	16.12	12.29	11.85	10.44	**94.69**
η_th/PU(%)	63.72	63.03	59.45	53.32	60.42	62.48	
η_th/plant(%)							252.51
SSI(%)							**152.51**
wnn(kJ/kg)=	**Total net work out = wn(SSPM)*CCF(SHSk) - wn(RBC)=**						**124.111**

Table 17 illustrates the set of 6 cascaded PUs operated by a VsVs cycle with Nitrogen as real TWF.

Table 17: Illustration of the 6-PU set operating in cascade. The data in the table corresponds to Nitrogen as the actual gas for the TWF.

PU1-N2	**T(K)**	**p(bar)**	**v(m3/kg)**	**u(kJ/kg)**	**s(kJ/kg.K)**
1	680.00	10.000	0.20267	511.22	7.025
2	800.00	11.770	0.20267	608.57	7.157
3	766.62	10.000	0.22830	580.69	7.157
4	651.00	8.494	0.22830	488.29	7.025
PU2-N2	**T(K)**	**p(bar)**	**v(m³/kg)**	**u(kJ/kg)**	**s(kJ/kg.K)**
1	578.00	10	0.17228	431.02	6.849
2	680.00	11.7730	0.17228	511.11	6.977

3	650.85	10	0.19386	487.72	6.977
4	552.50	8.4891	0.19386	411.44	6.849
PU3-N2	**T(K)**	**p(bar)**	**v(m^3/kg)**	**u(kJ/kg)**	**s(kJ/kg.K)**
1	491.30	10	0.14640	364.46	6.676
2	578.00	11.7770	0.14640	430.87	6.800
3	552.25	10	0.16460	411.11	6.800
4	469.30	8.4897	0.16460	347.92	6.676
PU4-N2	**T(K)**	**p(bar)**	**v(m^3/kg)**	**u(kJ/kg)**	**s(kJ/kg.K)**
1	417.61	10	0.12434	308.71	6.504
	491.30	11.7830	0.12434	364.28	6.627
3	469.04	10	0.13974	347.56	6.627
4	398.70	8.4884	0.13974	294.69	6.504
PU5-N2	**T(K)**	**p(bar)**	**v(m^3/kg)**	**u(kJ/kg)**	**s(kJ/kg.K)**
1	354.96	10	0.10551	261.62	6.333
	417.61	11.7920	0.10551	308.48	6.455
3	398.42	10	0.11859	294.27	6.455
4	338.00000	8.4649	0.11859	249.15	6.333
PU6-N2	**T(K)**	**p(bar)**	**v(m^3/kg)**	**u(kJ/kg)**	**s(kJ/kg.K)**
1	301.72	10	0.08942	221.62	6.162
	354.96	11.8040	0.08942	261.33	6.283
3	338.50	10	0.10055	249.26	6.283
4	288.00	8.4817	0.10055	211.62	6.162

Table 18 illustrates the results corresponding to a group of six cascaded PUs operated by a VsVs cycle with Nitrogen as real TWF.

Table 18: Illustration of the result set of 6 PUs operating in cascade with Nitrogen as the real gas used as TWF represented in Table 17

PU-N2	1	2	3	4	5	6	total
LF(%)	0.85	0.85	0.85	0.85	0.85	0.85	0.85
RF(%)	0.95	0.95	0.95	0.95	0.95	0.95	0.95
RIT*100	85.0	85.0	85.0	85.0	85.00	85.0	85.00
T2(K)	800.00	680.00	578.00	491.30	417.61	354.96	
T1(K)	680.00	578.00	491.30	417.61	354.96	301.72	
qi_12/PU(kJ/kg)	97.35	80.09	66.41	55.57	46.86	39.71	385.99
qo_34(kJ/kg)	92.40	76.28	63.19	52.87	45.12	37.64	367.50
q_recov(kJ/kg)	87.78	72.47	60.03	50.23	42.86	35.76	349.13
Tm_qrecov(kJ/kg)		601.68	510.78	433.87	368.21	313.25	
wn(kJ/kg)	41.03	34.70	29.31	24.82	21.54	17.82	**169.23**
η_th/PU(%)	42.15	43.32	44.14	44.67	45.98	44.88	
η_th/plant(%)							173.83
SSI(%)							**73.83**
wnn(kJ/kg)=	**Total net work out = wn(SSPM)*CCF(SHSk) - wn(RBC)=**						**79.442**

Table 19 illustrates the set of 6 cascaded PUs operated by a VsVs cycle with Air as real TWF.

Table 19: Illustration of the 6-PU set operating in cascade. The data in the table corresponds to Air as real gas for the TWF.

PU1-Air	**T(K)**	**p(bar)**	**v(m³/kg)**	**u(kJ/kg)**	**s(kJ/kg.K)**
1	680.00	1	1.95310	623.14	4.732
2	800.00	1.1765	1.95310	718.84	4.862
3	766.62	1	2.20190	691.89	4.862
4	650.7	0.8487	2.20190	600.31	4.732
PU2-Air	**T(K)**	**p(bar)**	**v(m³/kg)**	**u(kJ/kg)**	**s(kJ/kg.K)**
1	578.00	1	1.66010	544.50	4.560
2	680.00	1.1766	1.66010	623.13	4.685
3	650.85	1	1.86940	600.42	4.685
4	552.50	0.8488	1.86940	525.22	4.560
PU3-Air	**T(K)**	**p(bar)**	**v(m³/kg)**	**u(kJ/kg)**	**s(kJ/kg.K)**
1	491.30	1	1.4110	479.48	4.3917
2	578.00	1.1766	1.4110	544.48	4.5135
3	552.71	1	1.5875	525.36	4.5135
4	469.30	0.8490	1.5875	463.24	4.3917
PU4-Air	**T(K)**	**p(bar)**	**v(m³/kg)**	**u(kJ/kg)**	**s(kJ/kg.K)**
1	417.61	1	1.19930	425.33	4.226
	491.30	1.1766	1.19930	479.46	4.345
3	469.46	1	1.34830	463.34	4.345
4	398.70	0.8492	1.34830	411.59	4.226
PU5-Air	**T(K)**	**p(bar)**	**v(m³/kg)**	**u(kJ/kg)**	**s(kJ/kg.K)**
1	354.96	1	1.01920	379.88	4.061
	417.61	1.1767	1.01920	425.31	4.179
3	398.88	1	1.14550	411.70	4.179
4	338.70	0.84891	1.14550	368.17	4.061
PU6-Air	**T(K)**	**p(bar)**	**v(m³/kg)**	**u(kJ/kg)**	**s(kJ/kg.K)**
1	301.72	1	0.86603	341.53	3.897
	354.96	1.1768	0.86603	379.85	4.014
3	338.83	1	0.97277	368.24	4.014
4	286.00	0.84382	0.97277	330.27	3.897

Table 20 illustrates the results corresponding to a group of six cascaded PUs operated by a VsVs cycle with Air as real TWF.

Table 20: Illustration of the result set of 6 PUs operating in cascade with Air as the real gas used as TWF represented in Table 19

PU-Air	1	2	3	4	5	6	total
LF(%)	0.85	0.85	0.85	0.85	0.85	0.85	0.85

RF(%)	0.95	0.95	0.95	0.95	0.95	0.95	0.95
RIT*100	85.0	85.0	85.0	85.0	85.00	85.0	85.00
T2(K)	800.00	680.00	578.00	491.30	417.61	354.96	
T1(K)	680.00	578.00	491.30	417.61	354.96	301.72	
qi_12/PU(kJ/kg)	95.70	78.63	65.00	54.13	45.43	38.32	377.21
qo_34(kJ/kg)	91.58	75.20	62.12	51.75	43.53	37.97	362.15
q_recov(kJ/kg)	87.00	71.44	59.01	49.16	41.35	36.07	344.04
Tm_qrecov(kJ/kg)		601.68	511.01	434.08	368.79	312.42	
wn(kJ/kg)	40.20	33.91	28.55	24.11	20.45	18.47	**165.68**
η_th/PU(%)	42.00	43.12	43.93	44.54	45.01	48.19	
η_th/plant(%)							173.13
SSI(%)							**73.13**
wnn(kJ/kg)=	**Total net work out = wn(SSPM)*CCF(SHSk) - wn(RBC)=**						**617.296**

Table 21 illustrates the set of 6 cascaded PUs operated by a VsVs cycle with Carbon dioxide as real TWF.

Table 21: Illustration of the 6-PU set operating in cascade. The data in the table corresponds to CO2 as real gas for the TWF.

PU1-CO2	**T(K)**	**p(bar)**	**v(m3/kg)**	**u(kJ/kg)**	**s(kJ/kg.K)**
1	680.00	10.000	0.12839	757.85	3.112
2	800.00	11.785	0.12839	872.54	3.267
3	779.00	10.000	0.14720	852.22	3.267
4	661.50	8.483	0.14720	740.95	3.112
PU2-CO2	**T(K)**	**p(bar)**	**v(m^3/kg)**	**u(kJ/kg)**	**s(kJ/kg.K)**
1	578.00	10	0.10883	665.44	2.933
Tin_feed 2	680.00	11.7960	0.10883	757.57	3.080
3	661.00	10	0.12477	740.24	3.080
4	560.60	8.4593	0.12477	650.54	2.933
PU3-CO2	**T(K)**	**p(bar)**	**v(m^3/kg)**	**u(kJ/kg)**	**s(kJ/kg.K)**
1	491.30	10	0.09209	591.38	2.763
2	578.00	11.8120	0.09209	665.08	2.901
3	561.00	10	0.10544	650.57	2.901
4	476.00	8.4631	0.10544	579.21	2.763
PU4-CO2	**T(K)**	**p(bar)**	**v(m^3/kg)**	**u(kJ/kg)**	**s(kJ/kg.K)**
1	417.61	10	0.07768	532.14	2.601
	491.30	11.8370	0.07768	590.91	2.730
3	476.20	10	0.08846	578.93	2.730
4	404.00	8.5000	0.08846	522.14	2.601
PU5-CO2	**T(K)**	**p(bar)**	**v(m^3/kg)**	**u(kJ/kg)**	**s(kJ/kg.K)**
1	354.96	10	0.06519	484.65	2.445
	417.61	11.8810	0.06519	531.49	2.567

3	403.20	10	0.07482	520.98	2.567
4	341.60	8.3943	0.07482	475.68	2.445
PU6-CO2	**T(K)**	**p(bar)**	**v(m^3/kg)**	**u(kJ/kg)**	**s(kJ/kg.K)**
1	301.72	10	0.05419	446.23	2.295
	354.96	11.9600	0.05419	483.72	2.409
3	341.50	10	0.06238	474.78	2.409
4	289.70	8.3596	0.06238	438.97	2.295

Table 22 illustrates the results corresponding to a group of six cascaded PUs operated by a VsVs cycle with Carbon dioxide as real TWF.

Table 22: Illustration of the result set of 6 PUs operating in cascade with Carbon dioxide as the real gas used as TWF represented in Table 21

PU-CO2	**1**	**2**	**3**	**4**	**5**	**6**	**total**
LF(%)	0.85	0.85	0.85	0.85	0.85	0.85	0.85
RF(%)	0.95	0.95	0.95	0.95	0.95	0.95	0.95
RIT*100	85.0	85.0	85.0	85.0	85.00	85.0	85.00
T2(K)	800.00	680.00	578.00	491.30	417.61	354.96	
T1(K)	680.00	578.00	491.30	417.61	354.96	301.72	
qi_12/PU(kJ/kg)	114.69	92.13	73.70	58.77	46.84	37.49	423.62
qo_34(kJ/kg)	111.27	89.70	71.36	56.79	45.30	35.81	410.23
q_recov(kJ/kg)	105.71	85.22	67.79	53.95	43.04	34.02	389.72
Tm_qrecov(kJ/kg)		610.80	518.50	440.10	372.40	315.60	
wn(kJ/kg)	30.06	26.03	21.54	17.75	15.73	13.08	**124.19**
η_th/PU(%)	26.21	28.25	29.23	30.20	33.58	34.89	
η_th/plant(%)							108.28
SSI(%)							**8.28**
wnn(kJ/kg)=	**Total net work out = wn(SSPM)*CCF(SHSk) - wn(RBC)=**						**50.502**

5 Analysis of results and discussion

A summary of the four case studies concerning to SSPMs operating with Argon, Nitrogen, Air and Carbon dioxide as TWFs are considered and depicted in Table 23.

Table 23: Summary of results from tables 16, 18, 20 and 22 for Ar, N_2, Air, and CO_2 respectively

PU-Ar	1	2	3	4	5	6	total
wn(kJ/kg)	23.89	20.10	16.12	12.29	11.85	10.44	**94.69**
η_th/plant(%)							**252.51**
SSI(%)							**152.51**
wnn(kJ/kg)	**Total net work out = wn(SSPM)*CCF(SHSk) - wn(RBC)=**						**124.111**
PU-N2	1	2	3	4	5	6	total
wn(kJ/kg)	41.03	34.70	29.31	24.82	21.54	17.82	**169.23**
η_th/plant(%)							**173.83**
SSI(%)							**73.83**

wnn(kJ/kg)	**Total net work out = wn(SSPM)*CCF(SHSk) - wn(RBC)=**						**79.442**
PU-Air	1	2	3	4	5	6	total
wn(kJ/kg)	40.20	33.91	28.55	24.11	20.45	18.47	**165.68**
η_th/plant(%)							**173.13**
SSI(%)							**73.13**
wnn(kJ/kg)	**Total net work out = wn(SSPM)*CCF(SHSk) - wn(RBC)=**						**76.24**
PU-CO2	1	2	3	4	5	6	total
wn(kJ/kg)	30.06	26.03	21.54	17.75	15.73	13.08	**124.19**
η_th/plant(%)							**108.28**
SSI(%)							**8.28**
wnn(kJ/kg)	**Total net work out = wn(SSPM)*CCF(SHSk) - wn(RBC)=**						**50.502**

Table 24 illustrates the most relevant results concerning to SSPM and CC-based (RBS-SSPM) operating with Argon, Nitrogen, Air, and Carbon dioxide.

Table 24: Summary of main results for SSPMs and CC-based (RBS-SSPM)

	Ar	**N_2**	**Air**	**CO_2**
Net SSPM work (kJ/kg)	94.7	169,23	165.7	124.2
Self-Sufficient Index [SSI (%)]	152.5	73.8	73.13	8.28
Net CC-based (RBS-SSPM) work (kJ/kg)	124.1	79.44	76.24	50.5

With reference to the results illustrated in Tables 23 and 24 a concise analysis of the most relevant results is presented, highlighting key findings and performance analysis

5.1 Self-Sustaining Power Machines (SSPMs) Performance

Argon (Ar): Achieves the highest **Self-Sufficiency Index (SSI = 152.5%)**, indicating strong autonomous operation. However, it produces the **lowest net work output (94.7 kJ/kg)** due to its low specific heat capacity.

Nitrogen (N_2) & Synthetic Air (SA): Both exhibit similar performance (~73% SSI), with Nitrogen yielding slightly higher net work (169.23 kJ/kg vs. 165.7 kJ/kg for Air).

Carbon Dioxide (CO_2): Least efficient (SSI = 8.28%) due to its low adiabatic index (γ = 1.3) and specific heat, resulting in poor heat-work conversion.

5.2 Combined Cycle (CC) Performance (RBC+SSPM)

Argon-Argon CC: Delivers the **highest net work (124.1 kJ/kg)**, leveraging Argon's efficiency in both the Reversed Brayton Cycle (RBC) and SSPM.

Other TWFs (N_2, Air, CO_2): Net work drops significantly (79.44, 76.24, and 50.5 kJ/kg, respectively) due to lower efficiency in the RBC stage.

5.3 Thermodynamic Efficiency

Argon-based SSPM: Exceptional thermal efficiency (**252.51%**), attributed to its high adiabatic index (γ = 1.667), enabling efficient heat recovery.

CO_2-based SSPM: Lowest efficiency (**108.28%**) due to poor heat-work conversion properties.

5.4 Practical Implications for Mars

Best TWF Choice:

For SSPM alone: **Nitrogen (N_2)** balances efficiency (73.8% SSI) and work output (169.23 kJ/kg).

For Combined Cycle (CC): **Argon (Ar)** is optimal (124.1 kJ/kg net work) despite extraction challenges.

CO_2 Limitations: While abundant in Mars' atmosphere, its inefficiency makes it unsuitable for high-performance power systems.

6 General Conclusions

The objective of the paper has been to publish a preliminary design task to implement a group of machine prototypes capable of generating energy using the natural resources of Mars planet atmosphere.

This paper contributes with a groundbreaking advancement in thermodynamics by introducing SSPMs capable of operating without an external heat source or heat sink on Mars environment. The proposed machine functions as a HIS, challenging conventional thermodynamic principles, particularly the FLT and SLT. Achieving such milestones and contributions has required challenging the foundations of physics, particularly everything related to energy. Therefore the key findings and contributions include:

The proposed hybrid isolated system (HIS)**,** combining RBC and SSPM, successfully operates without external heat sources/sinks, defying traditional thermodynamics.

Argon is the best-performing TWF in CC configurations, whereas Nitrogen is preferable for standalone SSPMs due to better work output.

CO_2 is impractical for high-efficiency power generation despite its abundance on Mars.

This work demonstrates a viable pathway for in-situ resource utilization (ISRU) on Mars, with SSPMs offering a reliable, maintenance-free alternative to nuclear power for sustained exploration and colonization.

The theoretical and practical Implications undergo the following considered topics:

-- Reinterpretation of Thermodynamics: The findings necessitate revising the FLT and SLT to account for pull forces, contraction work, and hybrid isolated systems**.**

-- Energy Independence: The SSPM enables autonomous power generation without fuel or external heat exchange, with applications in extreme environments (e.g., deep space, radiation zones).

A great effort on further empirical validation, along with a broader scientific discourse, is required to integrate these findings into mainstream thermodynamics. Finally, it is noteworthy that this work seeks a paradigm shift in thermodynamics, urging the scientific community to reconsider fundamental principles based on empirical evidence. The SSPM represents a disruptive innovation with the potential to revolutionize energy systems by enabling self-sustaining and perpetual operation without traditional thermodynamic constraints.

The empirical validation performed through case studies in this work should be considered with caution, since it depends on the results derived from previous works published as references [12-14] and [16-18], although a rigorous validation through the implementation of prototypes is claimed. Therefore, if the work published in the references cited above does not satisfy or does not meet the expectations validated through rigorous studies without experimental testing, such a proposal will not be viable on Mars.

Final Note: The results validate the feasibility of SSPMs for Martian energy systems, with Argon and Nitrogen emerging as the most promising working fluids to supply on demand unlimited energy independently of any atmospheric or environmental condition. Continuous developing tasks should be considered, mainly focused on:

-- Implementation and validation of prototypes to achieve versatility according to available patents [19-21] that can be advantageously licensed to potential applicants

-- Optimization of TWF extraction methods and scaling prototypes for industrial deployment.

References

1. Steele1, L. G. Benning, R. Wirth, S. Siljeström, M. D. Fries, E. Hauri, P. G. Conrad, K. Rogers, J. Eigenbrode, A. Schreiber, A. Needham, J. H. Wang, F. M. McCubbin, D. Kilcoyne, Juan Diego Rodriguez Blanco. Organic synthesis on Mars by electrochemical reduction of CO2. Sci Adv. 2018 Oct 31; 4(10): eaat5118. https://doi.org/10.1126/sciadv.aat5118 retrieved from: https://pmc.ncbi.nlm.nih.gov/articles/PMC6209388/

2. Nina Kopacz, Maria Angela Corazzi, Giovanni Poggiali, Ayla von Essen, Vincent Kofman, Teresa Fornaro, Hugo van Ingen, Eloi Camprubi, Helen E. King, John Brucato, Inge Loes ten Kate. The photochemical evolution of polycyclic aromatic hydrocarbons and nontronite clay on early Earth and Mars. Icarus. Volume 394, April 2023, 115437; https://doi.org/10.1016/j.icarus.2023.115437; retrieved from: https://www.sciencedirect.com/science/article/pii/S0019103523000143 .

3. Christiane Heinicke, Leszek Orzechowski, Marlies Arnhof. Updated design concepts of the Moon and Mars Base Analog (MaMBA). IAC-18-F1.2.3. 69th International Astronautical Congress (IAC), Bremen, Germany, 1-5 October 2018. Retrieved from: https://www.iafastro.org/events/iac/iac-2018/. Copyright ©2018 by the International Astronautical Federation (IAF). All rights reserved

4. Elon Musk. Mars & Beyond. The Road To Making Humanity Multiplanetary Retrieved from: https://www.spacex.com/humanspaceflight/mars/

5. Magnet Architectures and Active Radiation Shielding Study (MAARSS). Final Report for NASA Innovative Advanced Concepts Phase II. Retrieved from: https://www.nasa.gov/wp-content/uploads/2017/07/niac_2012_phaseii_westover_radiationprotectionandarchitecture_tagged.pdf?emrc=4e9d26.

6. Kristine Ferrone, CharlesWillis, Fada Guan , Jingfei Ma , Leif Peterson and Stephen Kry. A Review of Magnetic Shielding Technology for Space Radiation. Radiation 2023, 3, 46–57. https://doi.org/10.3390/radiation3010005; Retrieved from: https://www.mdpi.com/journal/radiation

7. Author links open overlay panel S.A. Washburn, S.R. Blattnig, R.C. Singleterry, S.C. Westover. Active magnetic radiation shielding system analysis and key technologies. Life Sciences in Space Research. Volume 4,January 2015, Pages 22-34. https://www.doi.org/10.1016/j.lssr.2014.12.004 .

8. Ramon Ferreiro Garcia. Power Plants and Cycles: Advances and trends. Book (2020):

ISBN: 9789390431595; DOI:10.9734/bpi/mono/978-93-90431-59-5. https://www.researchgate.net/publication/347635047_Power_Plants_and_Cycles_Advances_and_Trends.

9. Ramon Ferreiro Garcia, Jose Carbia Carril. Combined Cycle Consisting of Closed Processes Based Cycle Powered by A Reversible Heat Pump that Exceed Carnot Factor. Journal of Advances in Physics, Volume 15, (2018), Pages: 6078-6100. ISSN: 2347-3487. DOI: 10.24297/jap.v15i0.8034.

10. Ramon Ferreiro Garcia. Study of the disruptive design of a thermal power plant implemented by several power units coupled in cascade. Energy Technol. 2023, 2300362 (1-17). Published by Wiley-VCH GmbH. DOI: https://doi.org/10.1002/ente.202300362.

11. Ramón Ferreiro Garcia. Efficient disruptive power plant-based heat engines doing work by means of strictly isothermal closed processes. Journal of Advances in Physics Vol 22 (2024), p 30.53, ISSN: 2347-3487. https://rajpub.com/index.php/jap/article/view/9587. DOI: https://doi.org/10.24297/jap.v15i0.9587.

12. Ramón Ferreiro Garcia. Design study of a disruptive self-powered power plant prototype. *JOURNAL OF ADVANCES IN PHYSICS*, Vol 22 (2024), p 62.92, ISSN: 2347-3487. https://rajpub.com/index.php/jap/article/view/9596. DOI: https://doi.org/10.24297/jap.v22i.9596.

13. Ramón Ferreiro Garcia. Prototyping a Disruptive Self-Sustaining Power Plant enabled to overcome Perpetual Motion Machines. *JOURNAL OF ADVANCES IN PHYSICS*, Vol. 22 (2024), p 141.178, ISSN: 2347-3487. https://rajpub.com/index.php/jap/article/view/963. DOI: https://doi.org/10.24297/jap.v22i.9633.

14. Ramón Ferreiro Garcia. Prototyping Self-Sustaining Power Machines with Cascaded Power Units Composed by Pulse Gas Turbines. *JOURNAL OF ADVANCES IN PHYSICS*, Vol. 22 (2024), p 141.178, ISSN: 2347-3487. https://rajpub.com/index.php/jap/article/view/9648. DOI: https://doi.org/10.24297/jap.v22i.9648

15. E. W. Lemmon, M. L. Huber, M. O. McLinden, NIST Reference Fluid Thermodynamic And Transport Properties - REFPROP Version 8.0, User's Guide, NIST, Boulder, CO. 2007.

16. Ramón Ferreiro Garcia. Prototyping disruptive self-sufficiency power machines composed by cascaded power units based on thermo-hydraulic actuators. *JOURNAL OF ADVANCES IN PHYSICS*, Vol 22 (2024), p 141.178, ISSN: 2347-3487. https://rajpub.com/index.php/jap/article/view/9662. DOI: https://doi.org/10.24297/jap.v22i.9662.

17. Ramón Ferreiro Garcia. How to violate the first law of thermodynamics with an ASE of Papain and Newcomen before it was stated by Clausius. *JOURNAL OF ADVANCES IN PHYSICS*, *23*, 9–27. (2025) https://doi.org/10.24297/jap.v23i.9706

18. Ramón Ferreiro Garcia. Self-Sustaining Power Machines enabled to operate without both heat sink and heat source. *JOURNAL OF ADVANCES IN PHYSICS*, Vol. *23*,. (2025) 42–74 ISSN: 2347-3487. https://doi.org/10.24297/jap.v23i.9727

19. Patent: Planta térmica con máquina de doble efecto, acumuladores térmicos, convección forzada y alimentación térmica reforzada con un ciclo Brayton inverso y procedimiento de operación. Thermal power plant with double-effect machine, thermal accumulators, forced convection and reinforced thermal supply with a reverse Brayton cycle and operating procedure. Ramon Ferreiro Garcia, Jose Carbia Carril. application number 201700667 and publication number 2 696 950 B2. Accessed at: https://consultas2.oepm.es/ceo/jsp/busqueda/busqRapida.xhtml;jsessionid=MDkG1OIa9BfQrxSiImwxtYlC.ConsultasC2.

20. Patent: Procedimiento de operación de una máquina alternativa de doble efecto con adición y extracción de calor y convección forzada. Operating procedure of a double-acting reciprocating machine with heat addition and extraction and forced convection and operating procedure. Jose Carbia Carril, Ramon Ferreiro Garcia, application number P201700718 and publication number 2 704 449 B2. Accessed at: https://consultas2.oepm.es/ceo/jsp/busqueda/busqRapida.xhtml;jsessionid=-wHy58sbfVYQutIYN8s0+JKK.ConsultasC1.

21. Patent: Planta termoeléctrica multiestructural policíclica y procedimientos de operación. Polycyclic multi-structure thermal power plant and operating procedures. Ramon Ferreiro Garcia, application number P202200035 and publication number 2 956 342 B2. Accessed at: https://consultas2.oepm.es/ceo/jsp/busqueda/busqRapida.xhtml;jsessionid=-wHy58sbfVYQutIYN8s0+JKK.ConsultasC1.